L-184

ARR No. L4J05a

NATIONAL ADVISORY COMMITTEE FOR AERONAUTICS

WARTIME REPORT

ORIGINALLY ISSUED
November 1944 as
Advance Restricted Report L4J05a

EXPERIMENTAL VERIFICATION OF THE RUDDER-FREE STABILITY THEORY FOR AN AIRPLANE MODEL EQUIPPED WITH RUDDERS HAVING NEGATIVE FLOATING TENDENCY AND NEGLIGIBLE FRICTION

Control surfaces

By Marion O. McKinney, Jr. and Bernard Maggin

Langley Memorial Aeronautical Laboratory
Langley Field, Va.

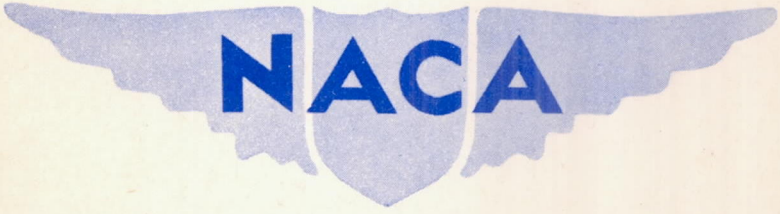

WASHINGTON

NACA ARR No. L4J05a

NATIONAL ADVISORY COMMITTEE FOR AERONAUTICS

ADVANCE RESTRICTED REPORT

EXPERIMENTAL VERIFICATION OF THE RUDDER-FREE STABILITY THEORY FOR AN AIRPLANE MODEL EQUIPPED WITH RUDDERS HAVING NEGATIVE FLOATING TENDENCY AND NEGLIGIBLE FRICTION

By Marion O. McKinney, Jr. and Bernard Maggin

SUMMARY

An investigation has been made in the Langley free-flight tunnel to obtain an experimental verification of the theoretical rudder-free stability characteristics of an airplane model equipped with conventional rudders having negative floating tendencies and negligible friction. The model used in the tests was equipped with a conventional single vertical tail having rudder area 40 percent of the vertical tail area. The model was tested both in free flight and mounted on a strut that allowed freedom only in yaw. Measurements were made of the rudder-free oscillations following a disturbance in yaw. Tests were made with three different amounts of rudder aerodynamic balance and with various values of mass, moment of inertia, and center-of-gravity location of the rudder. Most of the stability derivatives required for the theoretical calculations were determined from force and free-oscillation tests of the particular model tested.

The theoretical analysis showed that the rudder-free motions of an airplane consist largely of two oscillatory modes - a long-period oscillation somewhat similar to the normal rudder-fixed oscillation and a short-period oscillation introduced only when the rudder is set free. It was found possible in the tests to create lateral instability of the rudder-free short-period mode by large values of rudder mass parameters even though the rudder-fixed condition was highly stable.

The results of the tests and calculations indicated that, for most present-day airplanes having rudders of negative floating tendency, the rudder-free stability

characteristics may be examined by simply considering the dynamic lateral stability using the value of the directional-stability parameter C_{n_β} for the rudder-free condition in the conventional controls-fixed lateral-stability equations. For very large airplanes having relatively high values of the rudder mass parameters with respect to the rudder aerodynamic parameters, however, analysis of the rudder-free stability should be made with the complete equations of motion. Good agreement between calculated and measured rudder-free stability characteristics was obtained by use of the general rudder-free stability theory, in which four degrees of lateral freedom are considered.

When the assumption is made that the rolling motions alone or the lateral and rolling motions may be neglected in the calculations of rudder-free stability, it is possible to predict satisfactorily the characteristics of the long-period (Dutch roll type) rudder-free oscillation for airplanes only when the effective-dihedral angle is small. With these simplifying assumptions, however, satisfactory prediction of the short-period oscillation may be obtained for any dihedral. Further simplification of the theory based on the assumption that the rudder moment of inertia might be disregarded was found to be invalid because this assumption made it impossible to calculate the characteristics of the short-period oscillations.

INTRODUCTION

Some military airplanes have recently encountered dynamic instability in the rudder-free condition. Certain other airplanes have performed a rudder-free oscillation called "snaking" in which the airplane yaw and rudder motions are so coupled as to maintain a yawing oscillation of constant amplitude. These phenomena have been the subject of various theoretical investigations, and the factors affecting the rudder-free stability have been explored and defined in the theoretical analyses of references 1 to 3.

In reference 1 the most complete set of the three sets of equations of the rudder-free motion is developed. The equations of reference 1, however, are very involved and rather unwieldy, and use of these equations to

determine the rudder-free stability characteristics is consequently laborious. Such equations are usually simplified by neglecting certain degrees of freedom or certain parameters and thus obtaining approximate though satisfactorily accurate solutions.

In reference 2, the equations were simplified by neglecting the rolling motions of the airplane. In reference 3, which supersedes reference 2 for the rudder-free theory, further simplification was obtained by neglecting sidewise motion as well as rolling motion. An additional simplifying assumption of reference 3 is that the rudder moment of inertia might be neglected. It was realized that these simplified equations were not applicable throughout the entire range of the variables that could be obtained, but the results were believed to be generally applicable to airplanes of that period.

In order to obtain an experimental check of the general and simplified equations, an experimental program is being conducted in the Langley free-flight tunnel. The results of the first part of this program are reported herein and are concerned with the rudder-free dynamic stability of a $\frac{1}{7}$-scale airplane model in gliding flight equipped with rudders having inset-hinge balances and negligible friction.

The rudder-free stability characteristics of the model were investigated for varying amounts of rudder aerodynamic and mass balance. The model was tested both in free-flight and mounted on a strut that allowed freedom only in yaw in order to determine experimentally the differences caused by neglect of the rolling and lateral motions of an airplane with rudder free.

In order that the results obtained by theory and experiment might be correlated, calculations were made of the theoretical rudder-free stability of the model tested by equations involving four degrees of freedom and by equations involving fewer degrees of freedom. In addition, the rudder-free stability of the model was calculated by an approximate method that neglected all of the rudder parameters except those causing a reduction in the directional-stability parameter C_{n_β} for the rudder-free condition.

Various force, hinge-moment, and free-oscillation tests were run in order to determine as many as possible of the stability derivatives required in the calculations of rudder-free stability.

SYMBOLS

S	wing area, square feet
V	free-stream airspeed, feet per second
b	wing span, feet
c	wing chord, feet
b_r	span of rudder, feet
m	mass of model, slugs
m_r	mass of rudder, slugs
k_X	radius of gyration of model about longitudinal (X) axis, feet
k_Z	radius of gyration of model about vertical (Z) axis, feet
k_r	radius of gyration of rudder about hinge axis, feet
$\bar{x}_r$	distance from center of gravity of rudder system to hinge axis; positive when center of gravity is back of hinge, feet
l	distance from model center of gravity to rudder hinge line, feet
D	differential operator $\left(\frac{d}{ds}\right)$
s	distance traveled in spans (Vt/b)
P	period of oscillations, seconds
T	time required for motions to decrease to one-half amplitude, seconds
t	time, seconds

A, B, C, D, E coefficients of stability quartic for rudder-fixed lateral stability

A_1, B_1, C_1, D_1, E_1, F_1, G_1, H_1 coefficients of stability septic for rudder-free lateral stability

A_2, B_2, C_2, D_2, E_2, F_2 coefficients of stability quintic for rudder-free lateral stability

A_3, B_3, C_3, D_3, E_3 coefficients of stability quartic for rudder-free lateral stability

A_4, B_4, C_4, D_4, coefficients of stability cubic for rudder-free lateral stability

λ root of stability determinant ($\lambda = a' \pm ib'$)

ib' imaginary portion of complex root of stability quartic

a' real root or real portion of a complex root of stability quartic

q dynamic pressure, pounds per square foot $\left(\frac{1}{2}\rho V^2\right)$

ρ mass density of air, slug per cubic foot

μ model relative-density factor ($m/\rho Sb$)

μ_r rudder relative-density factor ($m_r/\rho b_r \bar{c}_r^2$)

$\bar{c}_r$ root-mean-square chord of rudder, feet

α angle of attack, radians unless otherwise defined

β angle of sideslip, radians unless otherwise defined

ϕ angle of roll, radians unless otherwise defined

ψ angle of yaw, radians unless otherwise defined

δ rudder angular deflection, radians unless otherwise defined

γ flight-path angle, radians unless otherwise defined

p rolling angular velocity, radians per second

r yawing angular velocity, radians per second

v lateral component of velocity, feet per second

C_L lift coefficient $\left(\frac{\text{Lift}}{qS}\right)$

C_D drag coefficient $\left(\frac{\text{Drag}}{qS}\right)$

C_m pitching-moment coefficient $\left(\frac{\text{Pitching moment}}{qSc}\right)$

C_Y lateral-force coefficient $\left(\frac{\text{Lateral force}}{qS}\right)$

C_l rolling-moment coefficient $\left(\frac{\text{Rolling moment}}{qSb}\right)$

C_n yawing-moment coefficient $\left(\frac{\text{Yawing moment}}{qSb}\right)$

C_h hinge-moment coefficient $\left(\frac{\text{Hinge moment}}{qb_r\bar{c}_r^2}\right)$

C_{Y_β} rate of change of lateral-force coefficient with angle of sideslip $(\partial C_Y/\partial\beta)$

C_{l_β} rate of change of rolling-moment coefficient with angle of sideslip $(\partial C_l/\partial\beta)$

C_{l_p} rate of change of rolling-moment coefficient with rolling angular-velocity factor $\left(\partial C_l/\partial\frac{pb}{2V}\right)$

C_{l_r} rate of change of rolling-moment coefficient with yawing angular-velocity factor $\left(\partial C_l/\partial\frac{rb}{2V}\right)$

C_{n_β} rate of change of yawing-moment coefficient with angle of sideslip $(\partial C_n/\partial\beta)$

C_{n_ψ} rate of change of yawing-moment coefficient with angle of yaw $\left(\frac{\partial C_n}{\partial \psi} = -C_{n_\beta}\right)$

C_{n_p} rate of change of yawing-moment coefficient with rolling angular-velocity factor $\left(\partial C_n / \partial \frac{pb}{2V}\right)$

C_{n_r} rate of change of yawing-moment coefficient with yawing angular-velocity factor $\left(\partial C_n / \partial \frac{rb}{2V}\right)$

C_{n_δ} rate of change of yawing-moment coefficient with rudder angular deflection $(\partial C_n / \partial \delta)$

C_{h_β} rate of change of rudder hinge-moment coefficient with angle of sideslip $(\partial C_h / \partial \beta)$

C_{h_ψ} rate of change of rudder hinge-moment coefficient with angle of yaw $\left(\frac{\partial C_h}{\partial \psi} = -C_{h_\beta}\right)$

C_{h_r} rate of change of rudder hinge-moment coefficient with yawing angular-velocity factor $\left(\partial C_h / \partial \frac{rb}{2V}\right)$

C_{h_δ} rate of change of rudder hinge-moment coefficient with rudder angular deflection $(\partial C_h / \partial \delta)$

$C_{h_{D\delta}}$ rate of change of rudder hinge-moment coefficient with rudder angular-velocity factor $\left[\partial C_h / \partial \left(\frac{d\delta}{dt}\frac{b}{2V}\right)\right]$

APPARATUS

The tests were run in the Langley free-flight tunnel, a complete description of which is given in reference 4. The model used in the tests was a modified 1/7-scale model of a Fairchild XPZK-1 airplane with its center of

gravity located 23.8 percent of the mean aerodynamic chord. Figure 1 is a three-view drawing of the model. The mass and dimensional characteristics of the model are given in the following table:

Weight, pounds	3.75
Radius of gyration, k_z, foot	0.784
Wing area, square feet	3.47
Wing span, feet	4.75
Wing chord, foot	0.785
Distance from airplane center of gravity to rudder hinge line, feet	2.07
Height of rudder, foot	0.667
Root-mean-square chord of rudder, foot	0.185

The vertical tail of the model was a straight-taper surface with a rudder of the inset-hinge type. The area of the rudder behind the hinge line was 40 percent of the vertical tail area. Three different nose balances were attached to the rudder in order to vary the amount of aerodynamic balance. Sketches of these surfaces are given in figure 2. The mass characteristics of the rudder were varied by moving weights within the rudder or along a thin metal strip that protruded at the base of the rudder trailing edge. The rudders were mounted on ball bearings to reduce friction to a minimum.

The yaw stand used in the tests was fixed to the tunnel floor and allowed the model complete freedom in yaw but restrained it from rolling or sidewise motions. A photograph of the model installed on the yaw stand is shown as figure 3.

TESTS

Tests were made to determine the period and damping of the rudder-free lateral oscillations of the model during free gliding flight and when mounted on the yaw stand. No tests were performed to determine the effect upon the rudder-free stability of eliminating only rolling motions.

Scope of Tests

The range of rudder aerodynamic and mass characteristics covered in the tests is given in table I. The test range investigated was obtained by altering the mass characteristics of the rudder by addition of weights at various locations. In this manner the mass, center of gravity, and radius of gyration of the rudder were varied simultaneously. This procedure was followed for the rudder equipped with each of three different amounts of aerodynamic balance. All tests were run at a dynamic pressure of 1.90 pounds per square foot, which corresponded to an airspeed of approximately 40 feet per second. The lift coefficient was approximately 0.6.

Flight Tests

Flight tests were made for the model test conditions 1 to 3 and 10 to 13 of table I. These tests were made by flying the test model freely within the tunnel as explained in reference 4. During a given flight, a mechanism within the model was so activated as to free the rudder after an abrupt rudder deflection of about 15°. The rudder-free lateral oscillations resulting from the rudder disturbance were recorded by a motion-picture camera. The period and damping characteristics of the flight oscillations were obtained from the motion-picture record and were correlated with corresponding records from the yaw-stand tests and with calculated characteristics. Several runs were made at each test condition and showed a variation of period of about 2 percent and a variation of damping of less than 10 percent. Typical flight oscillations are shown in figure 4(a) for a stable condition and in figure 4(b) for an unstable condition.

Yaw-Stand Tests

The yaw-stand tests were made for all test conditions listed in table I. These tests were made under conditions reproducing those considered in the analytical treatment of reference 3, in which the rolling and the lateral motion of the airplane center of gravity are neglected. For the yaw-stand tests, the model was attached to the stand and the rudder was deflected 15°. At the given test airspeed, the rudder was abruptly released and the resulting oscillations were photographed by means

of a motion-picture camera installed above the model. Records of the period and damping of the yawing oscillations were then obtained in the same manner as for flight tests. Approximately the same scatter of period and damping values was obtained in the yaw-stand tests as in the flight tests. Plots of representative yawing oscillations obtained from the yaw-stand tests are shown in figure 4(a) for a stable condition and in figure 4(b) for a neutrally stable condition.

Method of Analyzing Test Data

Stability theory indicates that the rudder-free lateral oscillations are composed of two superimposed oscillatory modes, one of which has a shorter period than the other. The test oscillations, however, after a short interval of time represented only one of these modes - the one that subsided later because of the period or damping. In general, the stability calculations showed that the short-period mode damped to one-half amplitude in roughly 1/50 the period of the other mode. The test oscillations therefore represented the long-period mode for most of the test conditions.

Measurement of Stability Derivatives

The stability derivatives necessary for the calculations are given on table II and were obtained by the following procedures: The partial derivatives of yawing-moment coefficient with respect to angle of yaw and rudder deflection, C_{n_ψ} and C_{n_δ}, were determined from force tests of the model on the six-component balance of the Langley free-flight tunnel described in reference 5. The results of these tests are presented in figures 5 to 8. The hinge-moment derivatives due to angle of yaw and rudder deflection, C_{h_ψ} and C_{h_δ}, were determined from hinge-moment tests of the model rudder, the data from which are presented in figures 9 to 11. The rudder hinge-moment derivative due to yawing angular velocity C_{h_r} was then calculated by the relationship

$$C_{h_r} = \frac{2l}{b} C_{h_\psi} \qquad (1)$$

The yawing-moment derivative due to yawing angular velocity C_{n_r} (fig. 12) was determined by the free-oscillation method described in reference 6, and the rudder hinge-moment derivative due to rudder angular velocity $C_{h_{D\delta}}$ was similarly determined. The measured values of the parameter $C_{h_{D\delta}}$ (-0.0236 for rudder 1 and -0.0424 for rudders 2 and 3) did not agree with the value of -0.142 as calculated by the method presented in reference 7 except that the frequency of the oscillation was neglected. The cause of this discrepancy was not determined but is believed to have been the high oscillation frequency at which the tests were run (about 6 cycles per second at an airspeed of 40 feet per second). This frequency corresponded approximately to the calculated frequency of the rudder in the rudder-free tests of conditions 1 to 9 in table II.

Measurements indicated that the frictional damping of the rudder was about one-tenth of the air damping. This value was considered negligible and no attempt was made to introduce friction derivatives into the calculations. Four runs were made with each rudder and the scatter of values of $C_{h_{D\delta}}$ was less than 10 percent.

The partial derivative of the rolling-moment coefficient with respect to the rolling velocity parameter C_{l_p} was determined from the charts of reference 8. The derivatives C_{l_r} and C_{n_p} were determined from the formulas given in reference 9.

CALCULATIONS

Scope

Calculations were made of the damping and period of the rudder-free lateral oscillations of the model for the range of airplane and rudder parameters given in table I. These calculations were made by equations that provided four degrees of freedom as well as the fewer degrees of freedom which resulted from the neglect of rolling or the neglect of rolling and lateral motions. Other calculations were made to determine the effect of varying the effective-dihedral parameter C_{l_β} upon the rudder-free stability characteristics.

Method

The customary methods of stability calculation (outlined in reference 3) were employed in the present investigation. The equations of motion were set up, rendered nondimensional, and so treated as to obtain the stability equations defining the period and damping of the lateral-stability modes.

Equations of motion.- The nondimensional equations of motion used in the calculations are given in the following paragraphs.

The equations used for the rudder-fixed condition are

$$\left.\begin{aligned}
&\left(2\mu D - C_{Y_\beta}\right)\beta + \left(-C_L\right)\phi + \left(2\mu D + C_L \tan\gamma\right)\psi = 0 \\
&\left(-C_{l_\beta}\right)\beta + \left[2\mu\left(\frac{k_X}{b}\right)^2 D^2 - \frac{1}{2}C_{l_p} D\right]\phi + \left(-\frac{1}{2}C_{l_r} D\right)\psi = 0 \\
&\left(-C_{n_\beta}\right)\beta + \left(-\frac{1}{2}C_{n_p} D\right)\phi + \left[2\mu\left(\frac{k_Z}{b}\right)^2 D^2 - \frac{1}{2}C_{n_r} D\right]\psi = 0
\end{aligned}\right\} \qquad (2)$$

Equations (2) yield the familiar lateral-stability equations of the form

$$A\lambda^4 + B\lambda^3 + C\lambda^2 + D\lambda + E = 0 \qquad (3)$$

The general equations of motion for the rudder-free condition (four degrees of freedom) are

$$\left.\begin{aligned}
&\left(2\mu D - C_{Y_\beta}\right)\beta + \left(-C_L\right)\phi + \left(2\mu D + C_L \tan\gamma\right)\psi = 0 \\
&\left(-C_{l_\beta}\right)\beta + \left[2\mu\left(\frac{k_X}{b}\right)^2 D^2 - \frac{1}{2}C_{l_p} D\right]\phi + \left(-\frac{1}{2}C_{l_r} D\right)\psi = 0 \\
&\left(-C_{n_\beta}\right)\beta + \left(-\frac{1}{2}C_{n_p} D\right)\phi + \left[2\mu\left(\frac{k_Z}{b}\right)^2 D^2 - \frac{1}{2}C_{n_r} D\right]\psi + \left(-C_{n_\delta}\right)\delta = 0 \\
&\left(-2\mu_r \frac{\bar{x}_r}{b} D - C_{h_\beta}\right)\beta \\
&\qquad + \left[2\mu_r\left(\frac{k_r}{b}\right)^2 D^2 - 2\mu_r \frac{\bar{x}_r}{b} D + 2\mu_r \frac{l\bar{x}_r}{b^2} D^2 - \frac{1}{2}C_{h_r} D\right]\psi \\
&\qquad\qquad + \left[2\mu_r\left(\frac{k_r}{b}\right)^2 D^2 - C_{h_\delta} - \frac{1}{2}C_{h_{D\delta}} D\right]\delta = 0
\end{aligned}\right\} \quad (4)$$

Equations (4) yield the rudder-free lateral-stability equations of the form

$$A_1\lambda^7 + B_1\lambda^6 + C_1\lambda^5 + D_1\lambda^4 + E_1\lambda^3 + F_1\lambda^2 + G_1\lambda + H_1 = 0 \quad (5)$$

For the rudder-free condition, when rolling is neglected (three degrees of freedom), the equations are

$$\left.\begin{aligned}
&\left(2\mu D - C_{Y_\beta}\right)\beta + \left(2\mu D\right)\psi = 0 \\
&\left(-C_{n_\beta}\right)\beta + \left[2\mu\left(\frac{k_Z}{b}\right)^2 D^2 - \frac{1}{2}C_{n_r} D\right]\psi + \left(-C_{n_\delta}\right)\delta = 0 \\
&\left(-2\mu_r \frac{\bar{x}_r}{b} D - C_{h_\beta}\right)\beta \\
&\qquad + \left[2\mu_r\left(\frac{k_r}{b}\right)^2 D^2 - 2\mu_r \frac{\bar{x}_r}{b} D + 2\mu_r \frac{l\bar{x}_r}{b^2} D^2 - \frac{1}{2}C_{h_r} D\right]\psi \\
&\qquad\qquad + \left[2\mu_r\left(\frac{k_r}{b}\right)^2 D^2 - C_{h_\delta} - \frac{1}{2}C_{h_{D\delta}} D\right]\delta = 0
\end{aligned}\right\} \quad (6)$$

Equations (6) yield stability equations of the form

$$A_2\lambda^5 + B_2\lambda^4 + C_2\lambda^3 + D_2\lambda^2 + E_2\lambda + F_2 = 0 \qquad (7)$$

When the rolling motion and the lateral motion of the center of gravity are neglected (two degrees of freedom), the equations are

$$\left.\begin{aligned}
&\left[2\mu\left(\frac{k_Z}{b}\right)^2 D^2 - \frac{1}{2}C_{n_r}D - C_{n_\psi}\right]\psi + \left(-C_{n_\delta}\right)\delta = 0 \\
&\left[2\mu_r\left(\frac{k_r}{b}\right)^2 D^2 + 2\mu_r\frac{i\bar{x}_r}{b^2}D^2 - \frac{1}{2}C_{h_r}D - C_{h_\psi}\right]\psi \\
&\qquad + \left[2\mu_r\left(\frac{k_r}{b}\right)^2 D^2 - C_{h_\delta} - \frac{1}{2}C_{h_{D\delta}}D\right]\delta = 0
\end{aligned}\right\} \qquad (8)$$

Equations (8) yield stability equations of the form

$$A_3\lambda^4 + B_3\lambda^3 + C_3\lambda^2 + D_3\lambda + E_3 = 0 \qquad (9)$$

If, in addition to neglect of rolling and lateral motion of the center of gravity, the rudder moment of inertia is also neglected, the equations are

$$\left.\begin{aligned}
&\left[2\mu\left(\frac{k_Z}{b}\right)^2 D^2 - \frac{1}{2}C_{n_r}D - C_{n_\psi}\right]\psi - \left(C_{n_\delta}\right)\delta = 0 \\
&\left(2\mu_r\frac{i\bar{x}_r}{b^2}D^2 - \frac{1}{2}C_{h_r}D - C_{h_\psi}\right)\psi + \left(-\frac{1}{2}C_{h_{D\delta}}D - C_{h_\delta}\right)\delta = 0
\end{aligned}\right\} \qquad (10)$$

Equations (10) yield stability equations of the form

$$A_4\lambda^3 + B_4\lambda^2 + C_4\lambda + D_4 = 0 \qquad (11)$$

Determination of period and damping of lateral oscillations.- The roots of equations (3), (5), (7), (9), and (11) are of the form $\lambda = a'$ or $\lambda = a' + ib'$. The roots are used in the following equations to determine the period and the time to damp to one-half amplitude:

$$P = \frac{2\pi}{b'}\frac{b}{V} \qquad (12)$$

and

$$T = \frac{-\log_e 0.5}{a'}\frac{b}{V} \qquad (13)$$

RESULTS AND DISCUSSION

The results of the tests and calculations are presented in table II, which lists the period and the reciprocal of the time to damp to one-half amplitude for each condition investigated. The reciprocal of the time to damp to one-half amplitude was chosen to evaluate the damping, because this value is a direct rather than an inverse measure of the degree of stability. Negative values of the reciprocal of the time to damp to one-half amplitude refer to the time to increase to double amplitude.

Correlation of Tests and General Equations

Calculations.- The stability calculations made with the general equations of motion indicated that the motions of an airplane with rudder free consist of two aperiodic modes (convergences or divergences) and two oscillatory modes, one of which is of a period 2 to 10 times the other. As shown by the results presented in table II, these calculations indicated that, as long as the rudder radius

of gyration and mass unbalance were small (conditions 1 to 9), the short-period mode was very heavily damped and, consequently, the characteristics of the more lightly damped long-period mode determined the nature of the rudder-free oscillations. Table II indicates also that the characteristics of the long-period mode were only slightly affected by the rudder parameters as long as the rudder mass parameters were low (conditions 1 to 9).

When the radius of gyration and the mass unbalance of the rudder were large (conditions 10 to 13), the calculated period of the short-period mode increased considerably and the damping decreased. At high negative floating ratios (conditions 12 and 13), the calculations indicated that the destabilizing effect of high rudder radius of gyration and mass unbalance was sufficient to cause lateral instability.

Flight tests.- The results of the flight tests are presented in table II. These data indicate that, for low values of the rudder mass parameters (conditions 1 to 9), the less damped and hence the apparent mode had a period of about 1.5 seconds, which corresponded to that calculated for the long-period mode. For high values of the rudder mass parameters (conditions 10 to 13), either the long- or the short-period mode was the less damped of the two modes and hence determined the characteristics of the apparent motion, depending upon the magnitude of the rudder aerodynamic parameters C_{h_β} and C_{h_δ}. For the condition of high rudder aerodynamic parameters (conditions 10 and 11) the long-period mode was the less damped. Condition 12, however, showed the short-period mode to be the less damped at somewhat lower values of the rudder mass parameters than those of condition 11, and condition 13 gave an unstable short-period oscillation for even lower values of rudder mass parameters.

Comparison of theoretical and calculated results.- The tests confirmed the results predicted by the theory inasmuch as an unstable lateral oscillation was obtained for test condition 13. The quantitative correlation of measured values of period and damping with corresponding values calculated by the use of the general equations is shown in figure 13. These data show that the agreement between measured and calculated values of period was excellent for all conditions tested. This agreement was also shown in the correlation between measured and calculated values of damping except for conditions 12 and 13.

For conditions 12 and 13, the calculations indicated a larger degree of instability than that encountered in the tests. This apparent discrepancy was explained by further calculations which showed that the rudder-free stability was critically dependent upon the rudder mass characteristics for these test conditions. The results of the further calculations are given in figure 14 and show that the degree of instability encountered in test condition 13 was indicated by theory to occur at somewhat smaller values of mass unbalance than that used for the tests. Another possible explanation of the discrepancy between tests and theory for conditions 12 and 13 is that the actual value of $C_{h_{p\delta}}$ for these low-frequency conditions might have been higher than the values used in the calculations and obtained from high-frequency measurements. More information is required to determine the effect of frequency of the oscillation on this parameter.

Physical interpretation.- In order to explain more clearly the physical aspects of the long- and short-period modes of the rudder-free oscillations, additional calculations were made of the rudder-free and rudder-fixed stability characteristics over a wide range of dihedral. In this way, it was possible to observe analytically the change of lateral stability with dihedral when the rudder was free.

A comparison of the results of the rudder-fixed and rudder-free calculations indicated that the short-period mode of the rudder-free oscillations had no counterpart in rudder-fixed flight (table II, condition 14). This mode, therefore, was an entirely new oscillation created by the new degree of freedom that occurred when the rudder was freed and probably represents the oscillation of the rudder about its own hinge line. The calculations also showed that the characteristics of the short-period mode were virtually independent of the effective-dihedral parameter C_{l_β}. The variation of the calculated values of period and damping of the short-period oscillation for condition 2 with the effective-dihedral parameter is as follows:

C_{l_β}	P (sec)	1/T (1/sec)
0	0.087	14.35
-.04	.087	14.35
-.08	.087	14.34
-.12	.087	14.34
-.16	.087	14.35

The additional calculations indicated that the characteristics of the long-period mode of rudder-free oscillations varied with the effective-dihedral parameter C_{l_β} in a manner similar to the variation of the rudder-fixed oscillations with this parameter. The results of these calculations are presented in figures 15 and 16 and indicate that the characteristics of the long-period mode for the rudder-free condition were of the same order as those of the rudder-fixed oscillation but were of lower damping and higher period. Inasmuch as freeing rudders of negative floating tendencies is known to decrease the directional-stability parameter C_{n_β} and a decrease in this factor is known to decrease the damping and to increase the period of the lateral oscillation (references 10 and 11), the long-period mode of the rudder-free oscillations appears to be a modification of the familiar Dutch roll oscillation normally encountered in controls-fixed flight. The characteristics of the long-period rudder-free mode may then be concluded to be largely dependent upon the same parameters as the rudder-fixed oscillatory mode. For airplanes having rudders of negative floating tendency, then, instability of the long-period rudder-free mode should occur at smaller values of effective dihedral than for the corresponding rudder-fixed condition.

Correlation of Tests and Simplified Equations

Neglect of rudder parameters.- Inasmuch as most present-day airplanes have low values of rudder mass parameters, the long-period mode is the predominant factor affecting the rudder-free stability characteristics for airplanes having rudders of negative floating tendency. Consideration of the rudder mass parameters would therefore not seem necessary for these airplanes. An approximate solution for the rudder-free stability has been obtained by simply considering the controls-fixed dynamic lateral-stability equations (2), in which the value of C_{n_β} for the rudder-free condition is used.

Calculations were made for the test conditions by this approximate method, and the period and damping results are presented in table II and, for condition 7, as points on figures 15 and 16. The value of C_{n_β} for

the rudder-free condition was calculated by the following relation from reference 1:

$$C_{n_\beta(\text{rudder free})} = C_{n_\beta(\text{rudder fixed})} - \frac{C_{h_\beta}}{C_{h_\delta}} C_{n_\delta}$$

The values of period and damping obtained with this method are in good agreement with the values calculated by the general equations for test conditions 1 to 9. For conditions 10 and 11 the correlation is rather poor, as was expected, because of the high values of rudder mass parameters at these two conditions. Because the approximate method cannot predict a short-period oscillation, this method failed completely to predict the important features of the rudder-free motions for conditions 12 and 13, for which the short-period oscillation was about neutrally damped. These calculations indicate that, although the predictions yielded by the approximate method are good at low values of the rudder mass parameters, a more complete analysis is necessary at high values of the rudder mass parameters.

Neglect of rolling motion.- The simplification obtained by neglecting rolling motion was investigated for the present report by comparing the results obtained by the general equations with those obtained by equations neglecting rolling (equation 6). The values of period and damping for the test conditions as calculated by equation (6) are presented in table II. In figure 17 the characteristics of the short-period mode obtained by this method are compared with those calculated by the general equations. The correlation of the characteristics of both the long- and short-period modes calculated by the modified equations with those obtained from flight tests or from calculations by the general equations is fair except for conditions 10 and 11. This fact might indicate that the simplified theory gives poor correlation for the case of near-neutral stability of the short-period mode when the period of the long- and short-period modes is nearly equal.

Equations (6) show that neglect of rolling eliminates all of the derivatives involving rolling moment as well as those involving rolling motions. The effect of C_{l_β}

on the lateral stability cannot, therefore, be predicted by this simplified method. The effect of dihedral on the long-period mode is to reduce both the period and the damping, as is shown in figures 15 and 16. For dihedral angles less than 5° $\left(C_{l_\beta} < 0.06\right)$, however, neglect of rolling in the equations gives conservative results, because these equations indicate less damping than the general equations for low values of rudder mass parameters (conditions 1 to 9). This result is obtained mainly because with low dihedral the rolling component of the motion is small.

The effect on the stability of neglect of rolling with rudder fixed has also been investigated. The results of these calculations are given in table II under condition 14 and show reasonably good agreement with the results obtained by the general theory for the rudder-fixed condition. This agreement is further proof that, for low values of dihedral, rolling may be neglected in making these calculations. On the other hand, for airplanes having high dihedral and large values of relative density and radii of gyration, the long-period oscillation might become unstable, as shown in references 10 and 11. The neglect of rolling for these conditions would invalidate the results for the condition with the rudder either free or fixed.

Neglect of rolling and lateral motion.- In the theoretical analysis of rudder-free stability published in reference 3, the equations were further simplified by neglecting lateral motion of the airplane center of gravity as well as the rolling motions. These simplified equations also predicted a long-period and a short-period oscillation.

Tests of the model in the rudder-free condition were made on the yaw stand in order to reproduce the theoretical assumptions made in reference 3 (freedom in yaw about the airplane Z-axis and freedom of the rudder about its hinge line). The results of these tests are presented in table II and indicate that, for low values of the rudder mass parameters (conditions 1 to 9), the long-period mode was the less damped and hence determined the characteristics of the apparent motion. For higher values of the rudder mass parameters (conditions 10 to 13), either the long- or short-period mode was the less damped, depending upon the magnitude of the rudder aerodynamic

parameters. For conditions 10 and 11, the long-period mode was the less damped; whereas, for conditions 12 and 13, neutral damping of the short-period mode was obtained at lower values of the rudder mass parameters.

It may be of interest to note that in unpublished data from yaw-stand tests, made at higher values of mass unbalance of the rudder than those presented herein, an unstable short-period oscillation was obtained. This unstable oscillation could be started with a very small disturbance and would increase in amplitude until it became a constant-amplitude oscillation of about $\pm 15^{\circ}$ yaw.

The results of calculations made by utilizing the equations of reference 3 are listed in table II and have been compared in figure 18 to measured values obtained from the yaw-stand tests. The data presented in figure 18 show that the equations of reference 3 closely predicted the rudder-free data obtained in the yaw-stand tests for stable conditions. Like the general theory, however, the simplified equations predicted instability of the short-period oscillation at lower values of rudder mass parameters than did the yaw-stand tests.

A comparison of the yaw-stand and free-flight test results shows that the elimination of the rolling and lateral motions results in somewhat longer period and less damping than is obtained in flight, as long as the long-period oscillation is the controlling factor in the apparent motion in flight. When the characteristics of the short-period oscillations are apparent in flight, tests on the yaw stand give nearly identical results with those from flight tests. These data indicate that for small effective dihedral angles neglect of the rolling and lateral motion yields conservative values for the long-period, rudder-free oscillation and accurate values for the short-period oscillation. This fact confirms the conclusion, drawn from the analytical investigation concerning the effect of dihedral, that the characteristics of the short-period mode are relatively independent of dihedral, which is a basic rolling derivative.

The data of table II indicate that the simplified theory of reference 3, which neglects rolling and lateral motion, predicted the characteristics of the short-period mode just as well as did the general theory and that use of the simplified theory was therefore justified in this respect.

Neglect of rolling, lateral motion, and rudder moment of inertia.- A further assumption suggested in reference 3 is that the moment of inertia of the rudder, in addition to rolling and lateral motion, might be disregarded in the calculation of rudder-free stability. The results of calculations made with the rudder moment of inertia neglected are presented in table II and indicate that, for airplanes with small amounts of effective dihedral, application of the theory gives a reasonably accurate prediction of the rudder-free stability characteristics as long as the long-period oscillation is the controlling factor in the apparent motion. For conditions in which the short-period oscillation is the less damped mode, however, the assumption must be considered wholly invalid for rudders of negative floating tendencies, because the calculations indicate that, when the rudder moment of inertia is neglected, the short-period mode is replaced by a heavily damped convergence.

CONCLUSIONS

The following conclusions were drawn from an investigation in the Langley free-flight tunnel of the rudder-free stability characteristics of an airplane model equipped with rudders of negative floating tendencies and having negligible friction:

1. For most present-day airplanes, consideration of the rudder mass parameters is not necessary in an analysis of the rudder-free stability characteristics. These characteristics may be examined simply by considering the dynamic lateral stability and by using the value of the directional-stability parameter C_{n_β} for the rudder-free condition in the conventional controls-fixed lateral-stability equations.

2. Analysis of the rudder-free stability of airplanes having relatively high values of the rudder mass parameters with respect to the rudder aerodynamic parameters (such as would be encountered in very large airplanes) should be made with the complete equations of motion for the rudder-free condition.

3. The rudder-free stability characteristics of the model tested were satisfactorily calculated when all four

degrees of lateral freedom were considered in the calculations.

4. The rudder-free characteristics of the model tested were predicted fairly well when rolling motions or rolling and lateral motions were neglected in the calculations. Instability of the rudder-free Dutch roll type oscillation, however, could not be predicted by this method.

5. Large amounts of rudder mass unbalance caused an unstable short-period rudder-free oscillation for the model tested.

6. The characteristics of the short-period oscillation are found to be independent of the airplane effective dihedral and were satisfactorily predicted for the model tested by either the general stability equations in which all four degrees of lateral freedom are considered or by the modified stability equations in which either the effects of rolling motions alone or of rolling motions and lateral motions of the airplane center of gravity are neglected.

7. When the rudder moment of inertia was neglected in the calculations, the characteristics of the short-period rudder-free oscillations for rudders having negative floating tendencies could not be predicted.

Langley Memorial Aeronautical Laboratory
National Advisory Committee for Aeronautics
Langley Field, Va.

REFERENCES

1. Bryant, L. W., and Gandy, R. W. G.: An Investigation of the Lateral Stability of Aeroplanes with Rudder Free. 4304, S. & C. 1097, British N.P.L., Dec. 18, 1939.

2. Jones, Robert T., and Cohen, Doris: An Analysis of the Stability of an Airplane with Free Controls. NACA Rep. No. 709, 1941.

3. Greenberg, Harry, and Sternfield, Leonard: A Theoretical Investigation of the Lateral Oscillations of an Airplane with Free Rudder with Special Reference to the Effect of Friction. NACA ARR, March 1943.

4. Shortal, Joseph A., and Osterhout, Clayton J.: Preliminary Stability and Control Tests in the NACA Free-Flight Wind Tunnel and Correlation with Full-Scale Flight Tests. NACA TN No. 810, 1941.

5. Shortal, Joseph A., and Draper, John W.: Free-Flight-Tunnel Investigation of the Effect of the Fuselage Length and the Aspect Ratio and Size of the Vertical Tail on Lateral Stability and Control. NACA ARR No. 3D17, 1943.

6. Campbell John P., and Mathews, Ward O.: Experimental Determination of the Yawing Moment Due to Yawing Contributed by the Wing, Fuselage, and Vertical Tail of a Midwing Airplane Model. NACA ARR No. 3F28, 1943.

7. Theodorsen, Theodore: General Theory of Aerodynamic Instability and the Mechanism of Flutter. NACA Rep. No. 496, 1935.

8. Pearson, Henry A., and Jones, Robert T.: Theoretical Stability and Control Characteristics of Wings with Various Amounts of Taper and Twist. NACA Rep. No. 635, 1938.

9. Bamber, Millard J.: Effect of Some Present-Day Airplane Design Trends on Requirements for Lateral Stability. NACA TN No. 814, 1941.

10. Campbell, John P., and Seacord, Charles L., Jr.: Effect of Wing Loading and Altitude on Lateral Stability and Control Characteristics of an Airplane as Determined by Tests of a Model in the Free-Flight Tunnel. NACA ARR No. 3F25, 1943.

11. Campbell, John P., and Seacord, Charles L., Jr.: The Effect of Mass Distribution on the Lateral Stability and Control Characteristics of an Airplane as Determined by Tests of a Model in the Free-Flight Tunnel. NACA ARR No. 3H31, 1943.

NATIONAL ADVISORY
COMMITTEE FOR AERONAUTICS

TABLE I.- TEST CONDITIONS

Test condition	Rudder	C_{h_δ}	C_{h_ψ}	$C_{h_{D\delta}}$	C_{h_r}	C_{n_δ}	μ_r	$\bar{x}_r/\bar{c}_r$	$\bar{x}_r/b$	$k_r/\bar{c}_r$	k_r^2
1	1	-0.390	-0.172	-0.0236	-0.1496	-0.0396	22.37	0.061	0.00282	0.408	0.000355
2	1	-.390	-.172	-.0236	-.1496	-.0396	16.39	.167	.00773	.267	.000153
3	1	-.390	-.172	-.0236	-.1496	-.0396	22.89	.308	.01422	.466	.000465
4	2	-.264	-.092	-.0424	-.0789	-.0498	27.30	0	0	.185	.000073
5	2	-.264	-.092	-.0424	-.0789	-.0498	27.30	.055	.00253	.185	.000073
6	2	-.264	-.092	-.0424	-.0789	-.0498	27.30	.110	.00507	.185	.000073
7	3	-.172	-.092	-.0424	-.0789	-.0516	27.30	0	0	.185	.000073
8	3	-.172	-.092	-.0424	-.0789	-.0516	27.30	.055	.00253	.185	.000073
9	3	-.172	-.092	-.0424	-.0789	-.0516	27.30	.110	.00507	.185	.000073
10	1	-.390	-.172	-.0236	-.1496	-.0396	29.13	.550	.02545	.755	.001225
11	1	-.390	-.172	-.0236	-.1496	-.0396	34.57	.710	.03280	.882	.001670
12	2	-.264	-.092	-.0424	-.0789	-.0498	36.40	.614	.02840	.950	.001785
13	3	-.172	-.092	-.0424	-.0789	-.0516	31.20	.467	.02160	.769	.001272
14	Rudder fixed										

For all tests the following parameters were held constant:

$\mu = 3.12$

$\left(\frac{k_Z}{b}\right)^2 = 0.0524$

$\left(\frac{k_X}{b}\right)^2 = 0.0273$

$l/b = 0.435$

$\gamma = 7°$

$C_{n_\psi} = -0.0842$

$C_{n_r} = -0.1126$

$C_L = 0.6$

$C_{l_\beta} = +0.0426$

$C_{l_p} = -0.45$

$C_{l_r} = 0.166$

$C_{n_p} = -0.0173$

$C_{Y_\beta} = -0.406$

TABLE II.- COMPARISON OF PERIOD AND DAMPING FROM FLIGHT AND YAW-STAND TESTS AND CALCULATIONS

Test condition[a]		Tests		Calculations				
		Flight	Yaw stand	General theory	Rolling neglected	Rolling and sideslip neglected	Rolling, sideslip, and moment of inertia neglected	Rudder parameters neglected[b]
Long-period oscillation								
1	Period, P	1.72	1.80	1.69	1.56	1.66	1.67	1.60
	Damping, 1/T	1.17	.90	1.12	.84	.92	.93	1.39
2	Period, P	1.61	1.78	1.60	1.60	1.65	1.65	1.60
	Damping, 1/T	1.09	.90	1.10	1.27	.88	.94	1.39
3	Period, P	1.48	1.66	1.40	1.70	1.60	1.61	1.60
	Damping, 1/T	1.06	1.00	1.10	1.32	.98	1.00	1.39
4	Period, P	----	1.69	1.60	1.70	1.68	1.68	1.60
	Damping, 1/T	----	.90	1.38	1.26	.93	.93	1.39
5	Period, P	----	1.65	1.56	1.60	1.65	1.66	1.60
	Damping, 1/T	----	.90	1.39	1.30	.96	.96	1.39
6	Period, P	----	1.62	1.56	1.60	1.62	1.62	1.60
	Damping, 1/T	----	1.00	1.41	1.26	.99	.99	1.39
7	Period, P	----	1.86	1.74	1.80	1.83	1.82	1.74
	Damping, 1/T	----	.90	1.33	1.20	.88	.88	1.39
8	Period, P	----	1.79	1.63	1.74	1.78	1.77	1.74
	Damping, 1/T	----	.90	1.35	1.26	.92	.99	1.39
9	Period, P	----	1.72	1.53	1.60	1.73	1.72	1.74
	Damping, 1/T	----	1.00	1.30	1.30	.97	.97	1.39
10	Period, P	1.30	1.60	1.20	1.50	1.49	1.50	1.60
	Damping, 1/T	.90	1.05	.92	1.43	1.03	1.14	1.39
11	Period, P	1.15	1.50	1.05	1.20	1.35	1.41	1.60
	Damping, 1/T	.87	1.20	.90	1.53	1.23	1.30	1.39
12	Period, P	----	----	0.96	0.99	1.08	1.16	1.60
	Damping, 1/T	----	----	5.30	5.80	3.85	1.74	1.39
13	Period, P	----	----	0.97	0.98	1.15	1.24	1.74
	Damping, 1/T	----	----	5.22	5.19	3.60	1.60	1.39
14	Period, P	----	1.56	1.30	1.66	1.50	----	----
	Damping, 1/T	----	1.00	1.87	1.44	1.05	----	----
Short-period oscillation								
1	Period, P	-----	----	0.16	----	0.15	---	
	Damping, 1/T	-----	----	5.66	----	4.92	400	
2	Period, P	-----	----	0.09	0.09	0.08	---	
	Damping, 1/T	-----	----	15.15	14.35	14.16	384	
3	Period, P	-----	----	0.20	0.18	0.12	---	
	Damping, 1/T	-----	----	4.43	3.40	3.46	370	
4	Period, P	-----	----	0.10	0.10	0.10	---	
	Damping, 1/T	-----	----	32.30	30.80	32.30	152	
5	Period, P	-----	----	0.10	0.10	0.10	---	
	Damping, 1/T	-----	----	32.30	30.80	32.20	147	
6	Period, P	-----	----	0.10	0.10	0.10	---	
	Damping, 1/T	-----	----	32.30	30.80	32.20	141	
7	Period, P	-----	----	0.12	0.12	0.12	---	
	Damping, 1/T	-----	----	32.30	30.80	32.20	99	
8	Period, P	-----	----	0.13	0.13	0.13	---	
	Damping, 1/T	-----	----	32.30	30.80	32.20	94	
9	Period, P	-----	----	0.13	0.13	0.13	---	
	Damping, 1/T	-----	----	32.50	30.80	32.20	88	
10	Period, P	-----	----	0.80	0.37	0.36	---	
	Damping, 1/T	-----	----	1.90	.88	.76	322	
11	Period, P	-----	----	0.87	0.52	0.51	---	
	Damping, 1/T	-----	----	1.56	.47	.44	278	
12	Period, P	0.83	0.88	0.88	0.91	0.90	---	
	Damping, 1/T	.10	.00	-3.31	-2.73	-1.82	71	
13	Period, P	0.92	0.90	0.88	0.92	0.84	---	
	Damping, 1/T	-.15	.00	-2.76	-2.19	-.94	45	
14	Period, P	-----	----	-----	-----	-----	---	
	Damping, 1/T	-----	----	-----	-----	-----	---	

[a] P and T given in seconds.

[b] Approximate method, all rudder parameters neglected except those affecting C_{n_β}.

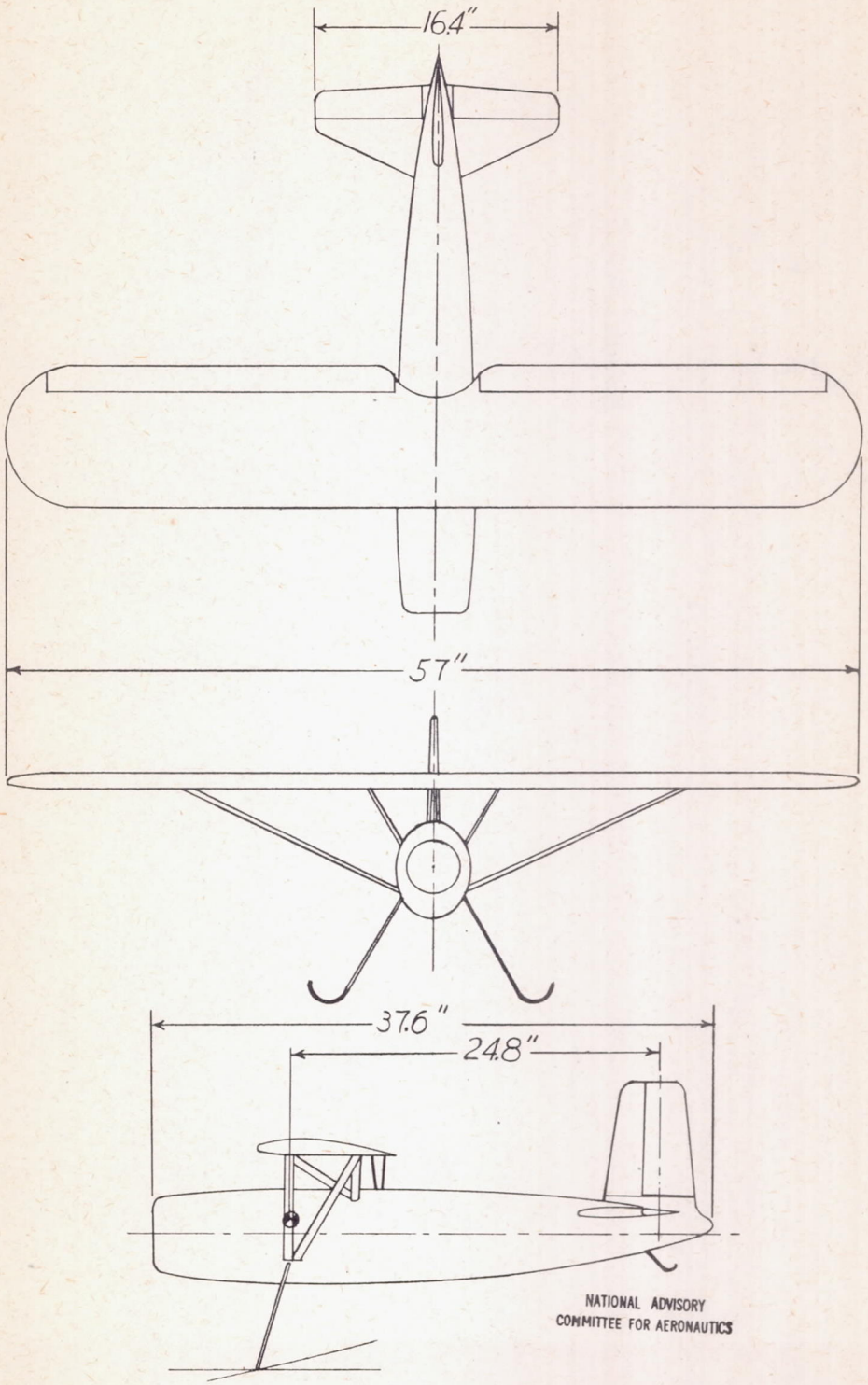

Figure 1.- Three-view drawing of the modified $\frac{1}{7}$-scale model of the Fairchild XR2K-1 airplane.

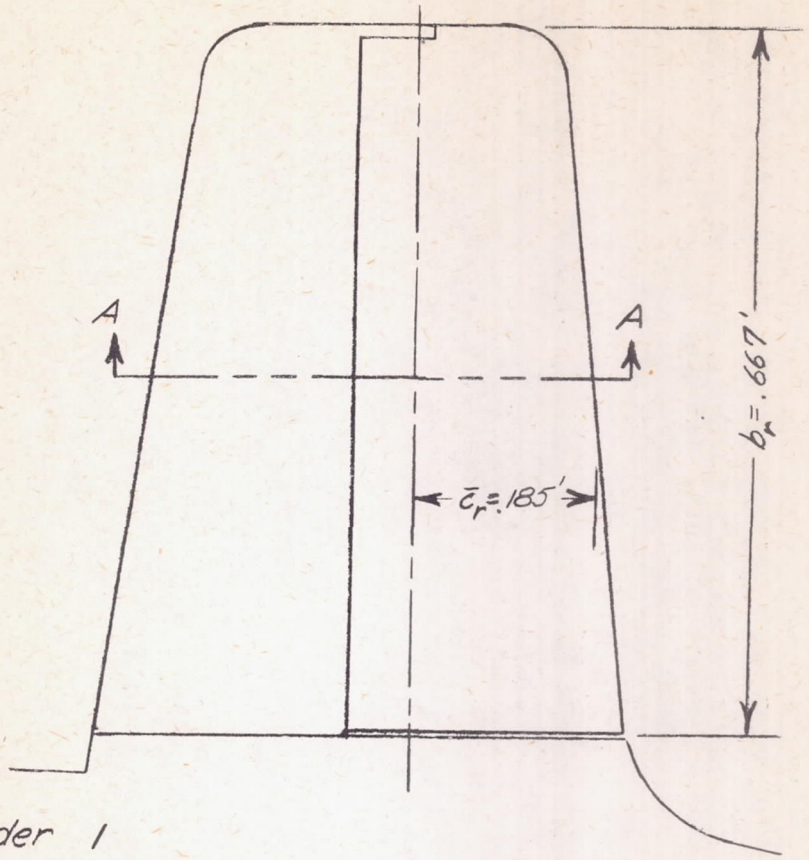

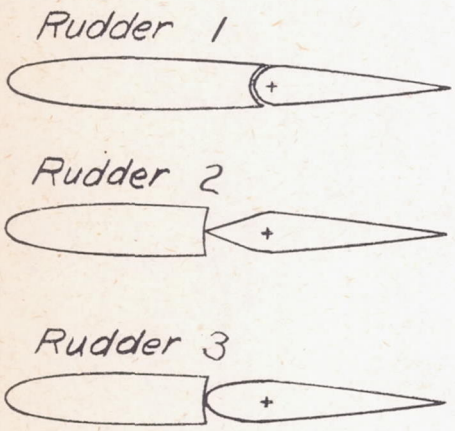

Sections A-A

Rudder	Rudder area in percent vertical-tail area	Balance in percent rudder area
1	40	0
2	40	35
3	40	35

NATIONAL ADVISORY COMMITTEE FOR AERONAUTICS

Figure 2. – Sketch of rudders used in the rudder-free stability investigation in the Langley free-flight tunnel.

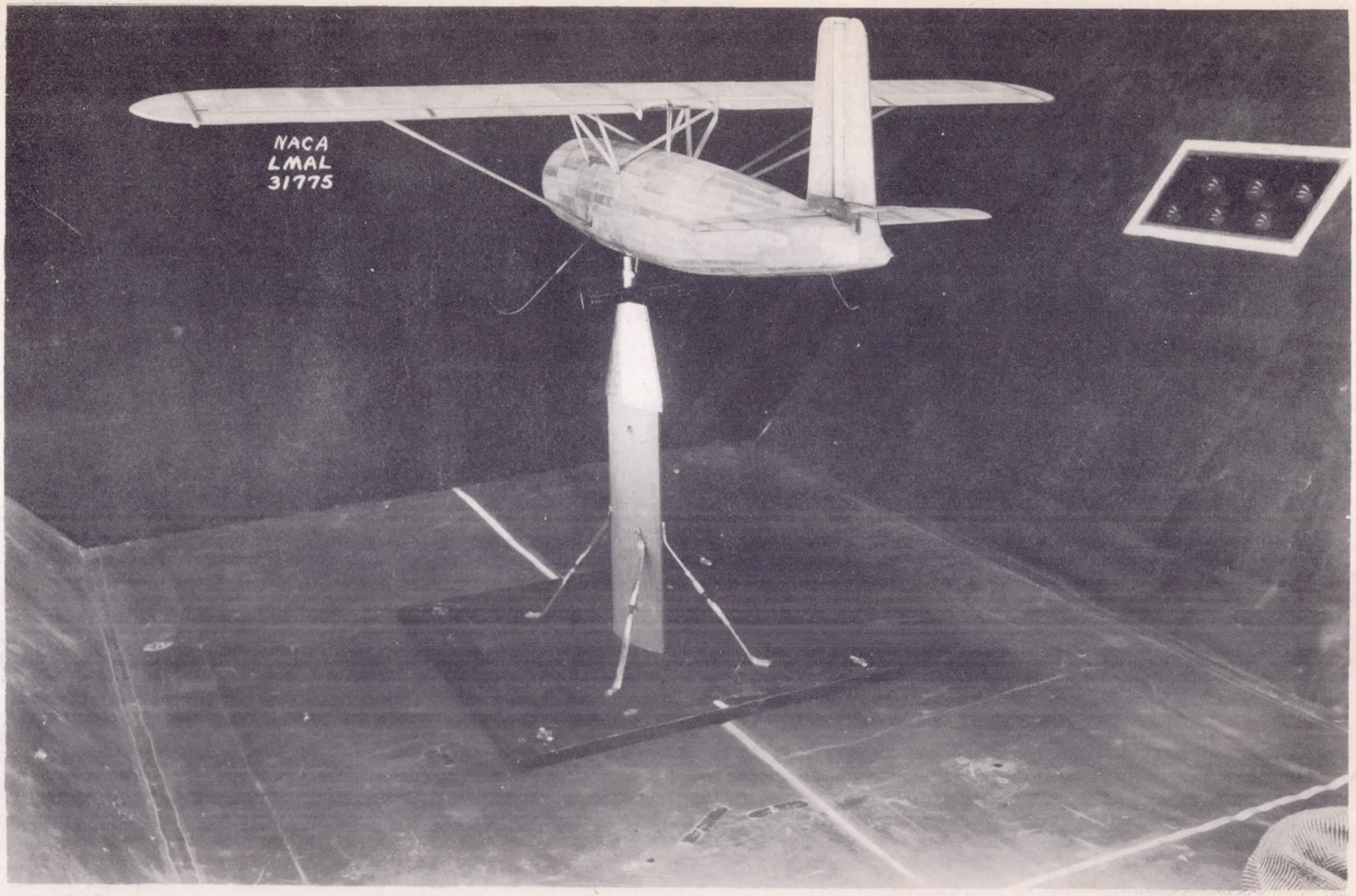

Figure 3.- Three-quarter rear view of $\frac{1}{7}$ -scale model of modified Fairchild XR2K-1 airplane mounted on yaw stand in Langley free-flight tunnel.

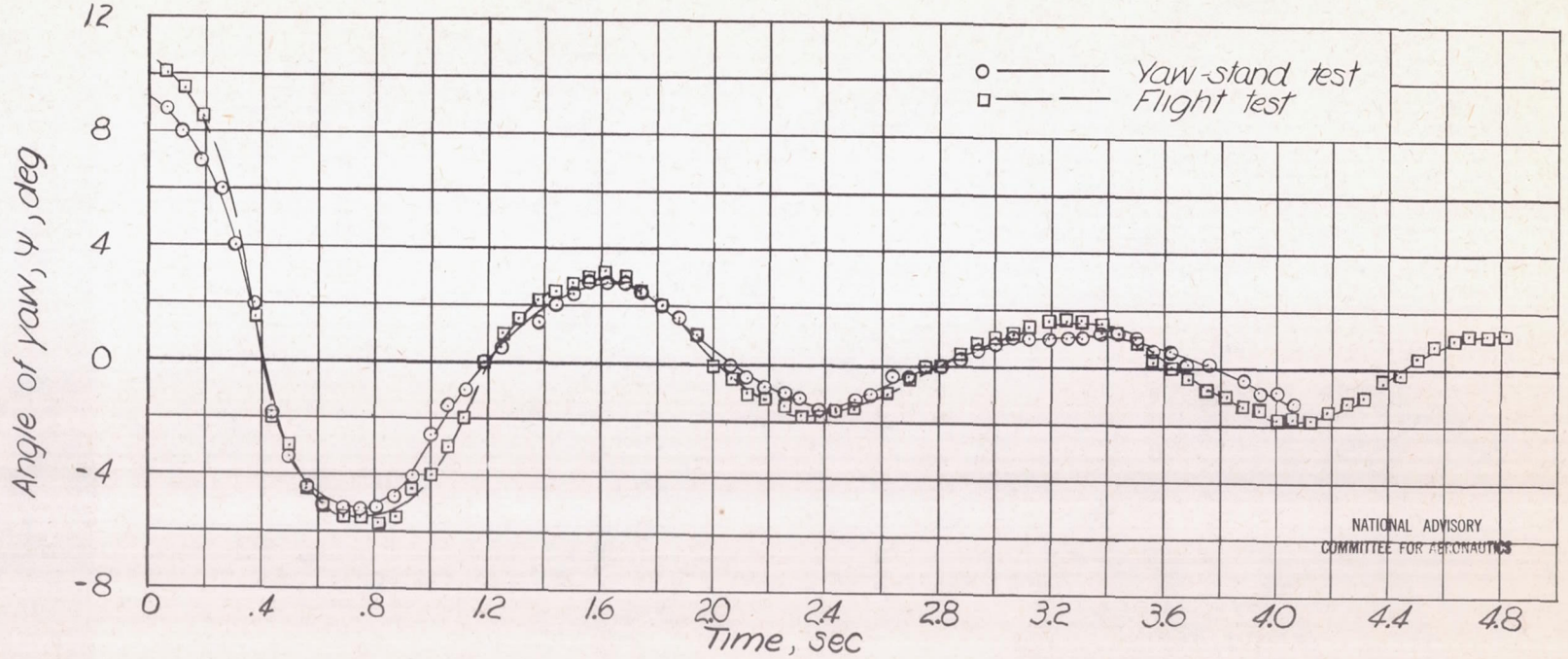

(a) Condition 10.

Figure 4.— Comparison of the rudder-free motion from flight and yaw-stand tests for a stable condition.

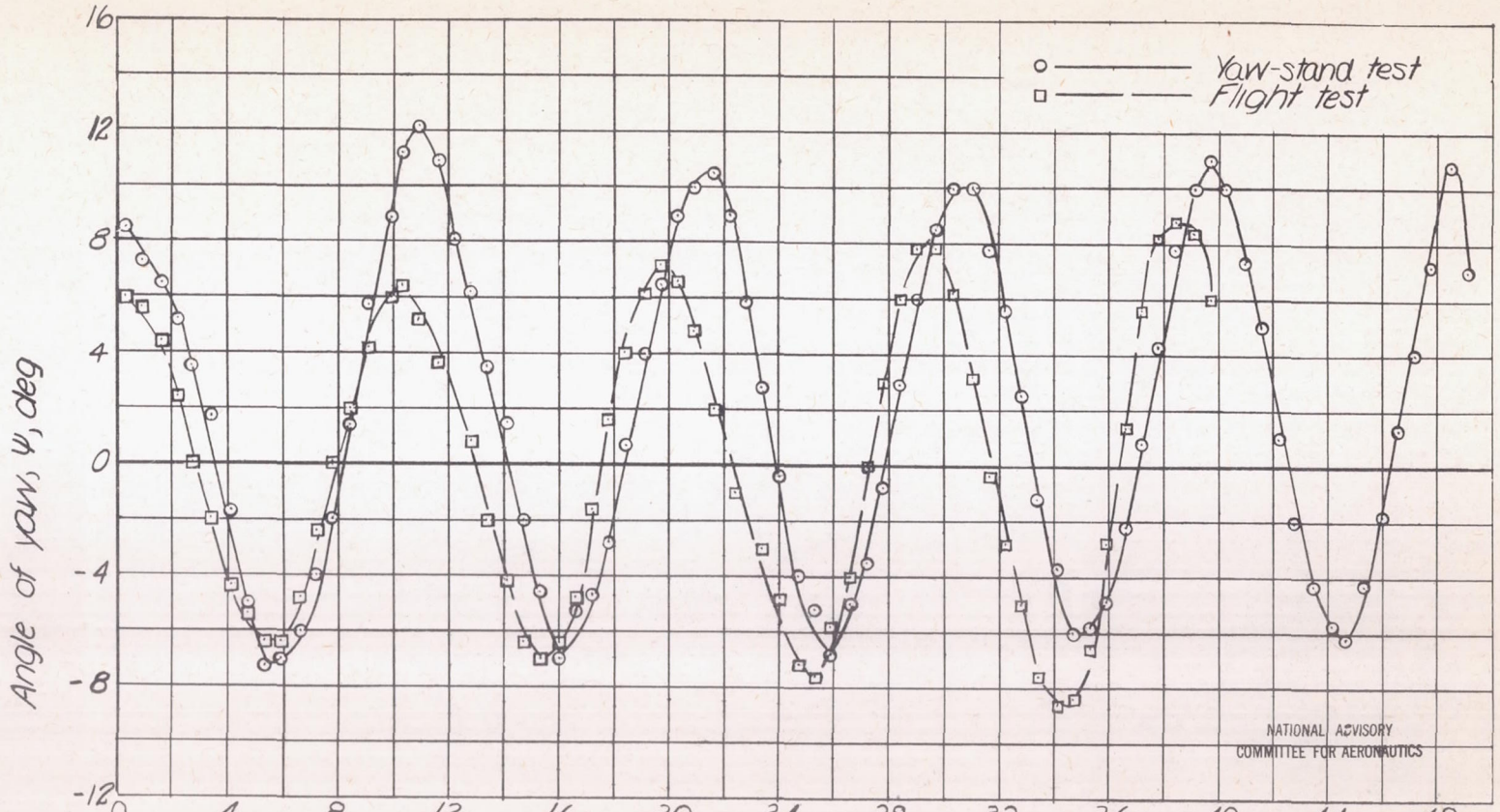

(b) Condition 13.

Figure 4.- Concluded.

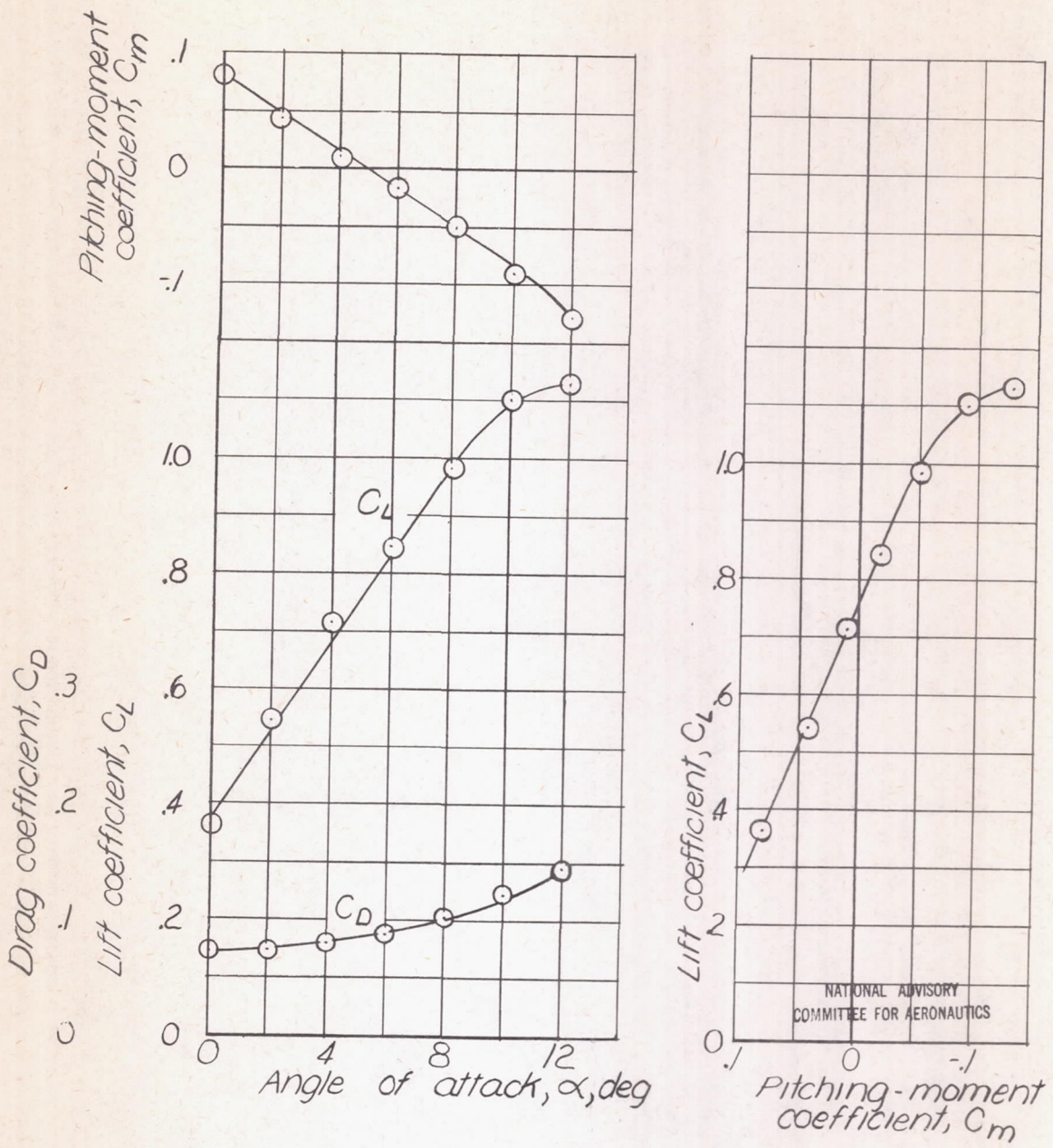

Figure 5.—Aerodynamic characteristics of the model used in the free-flight-tunnel investigation of rudder-free stability.

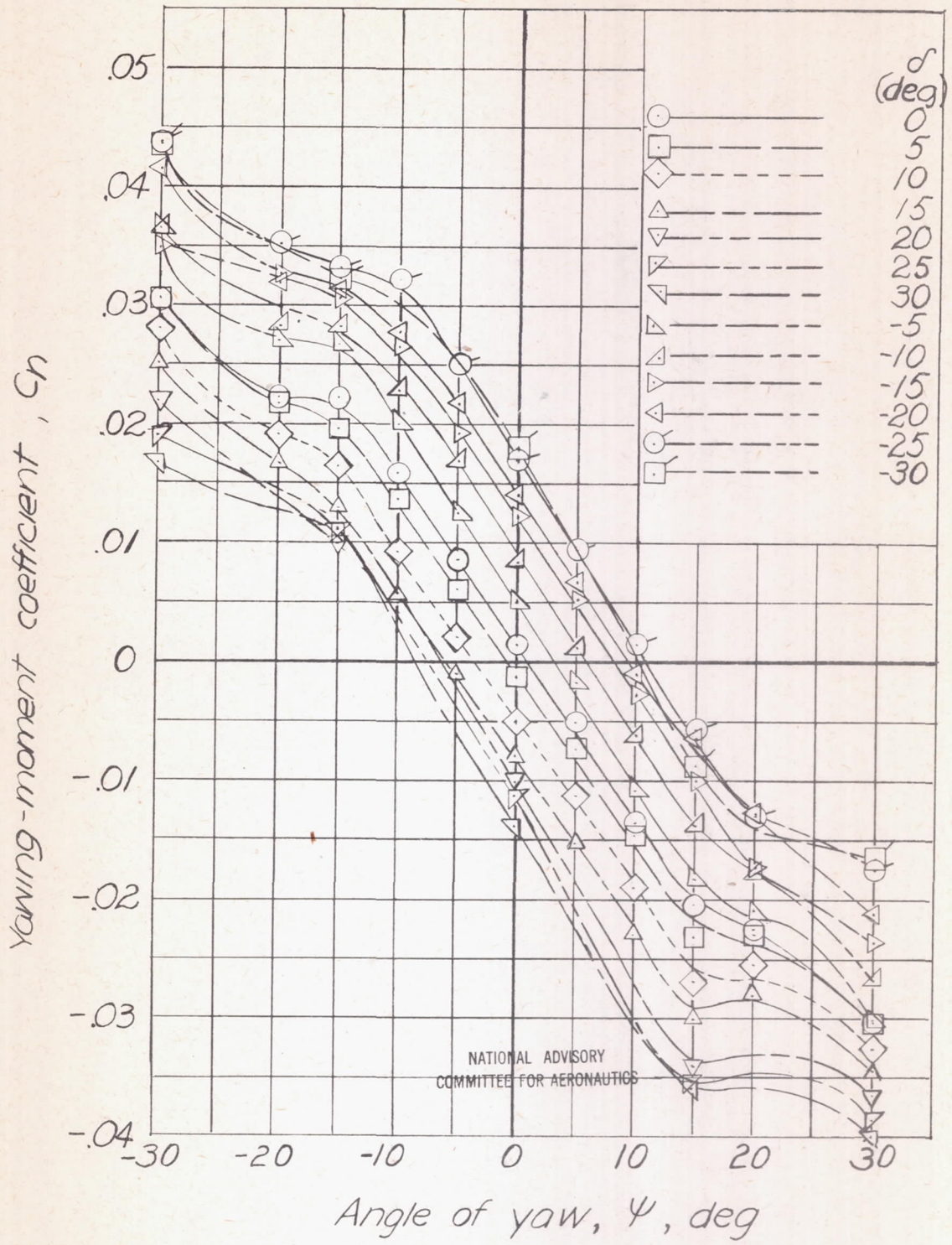

Figure 6.- Rudder effectiveness for rudder 1.

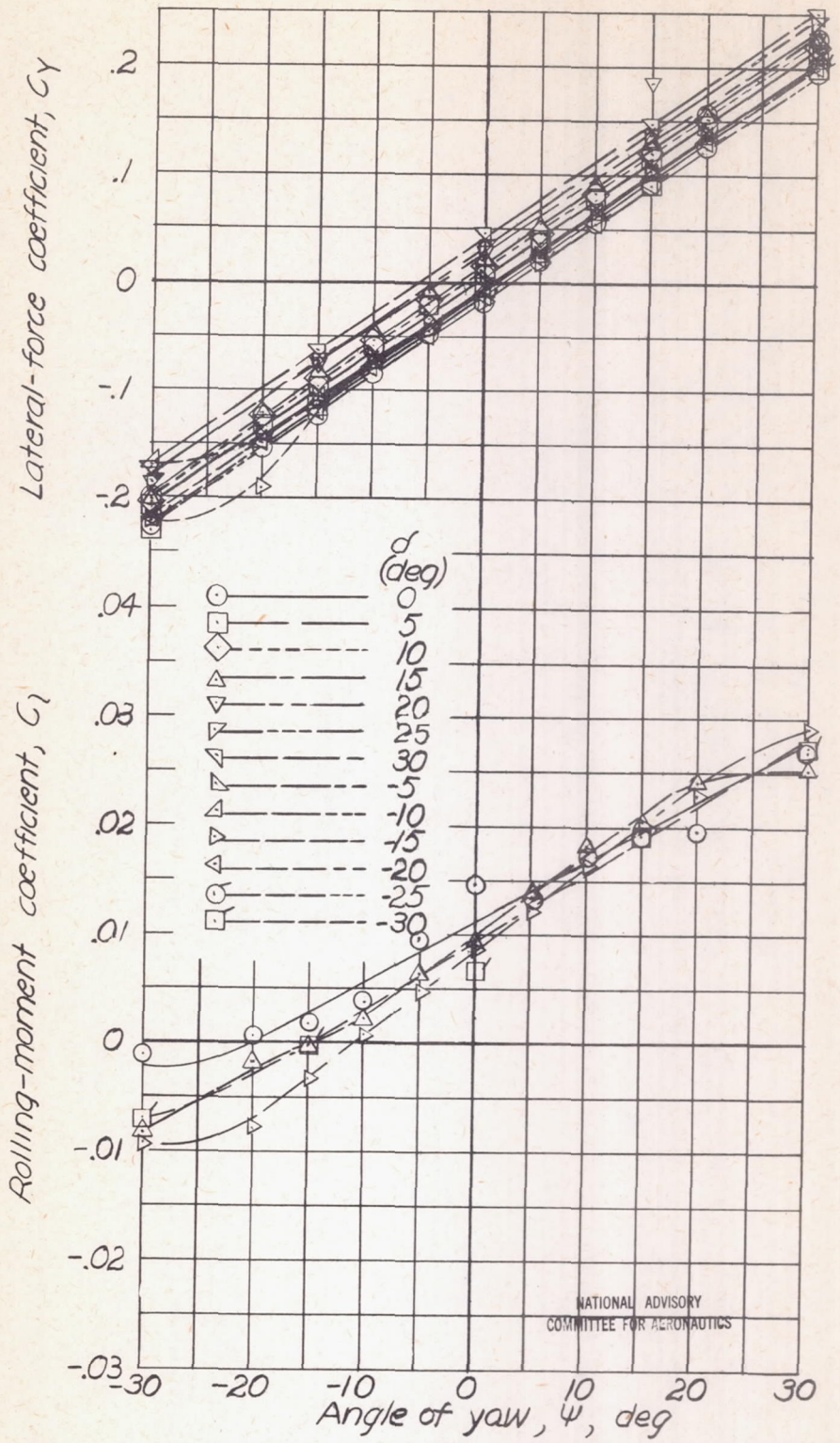

Figure 6.- Concluded.

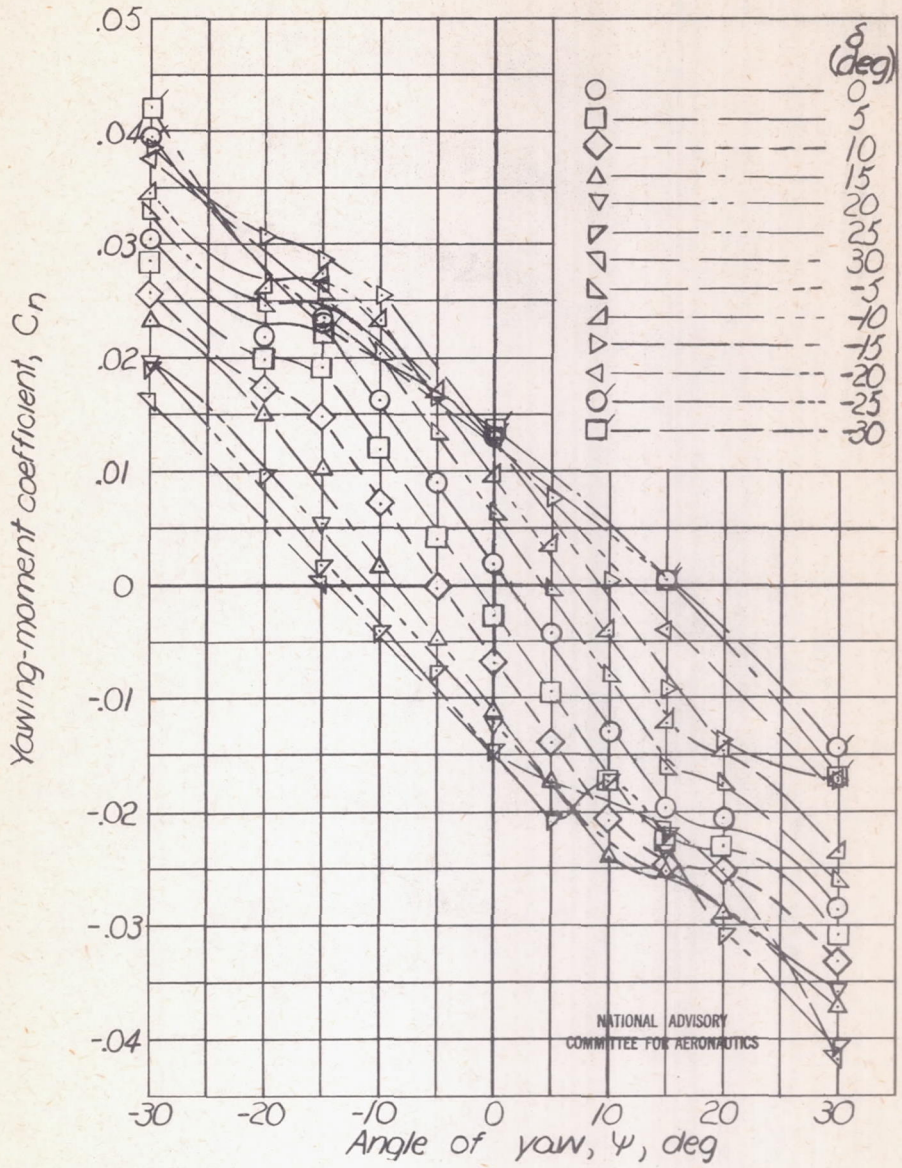

Figure 7.- Rudder effectiveness for rudder 2.

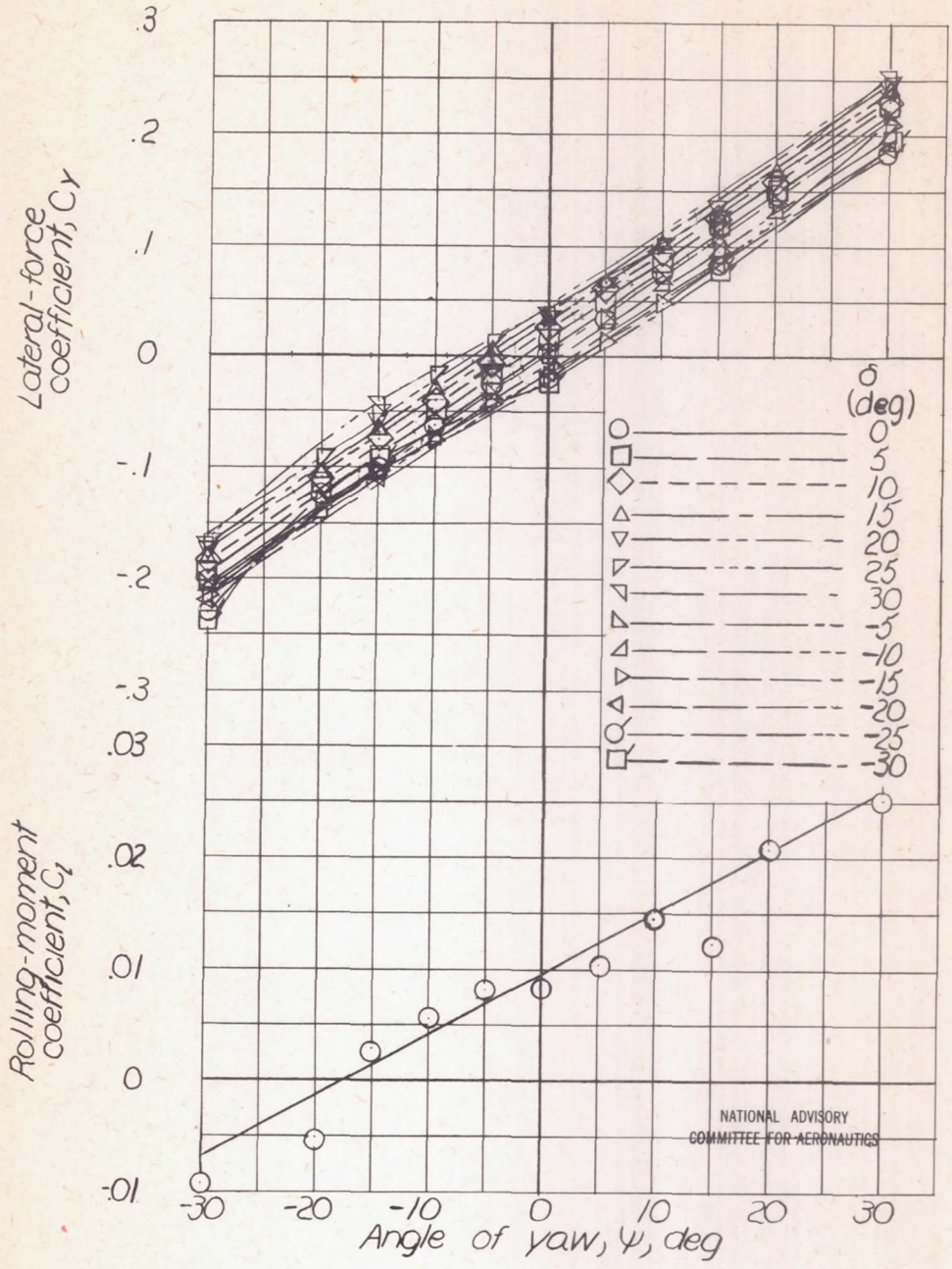

Figure 7.- Concluded.

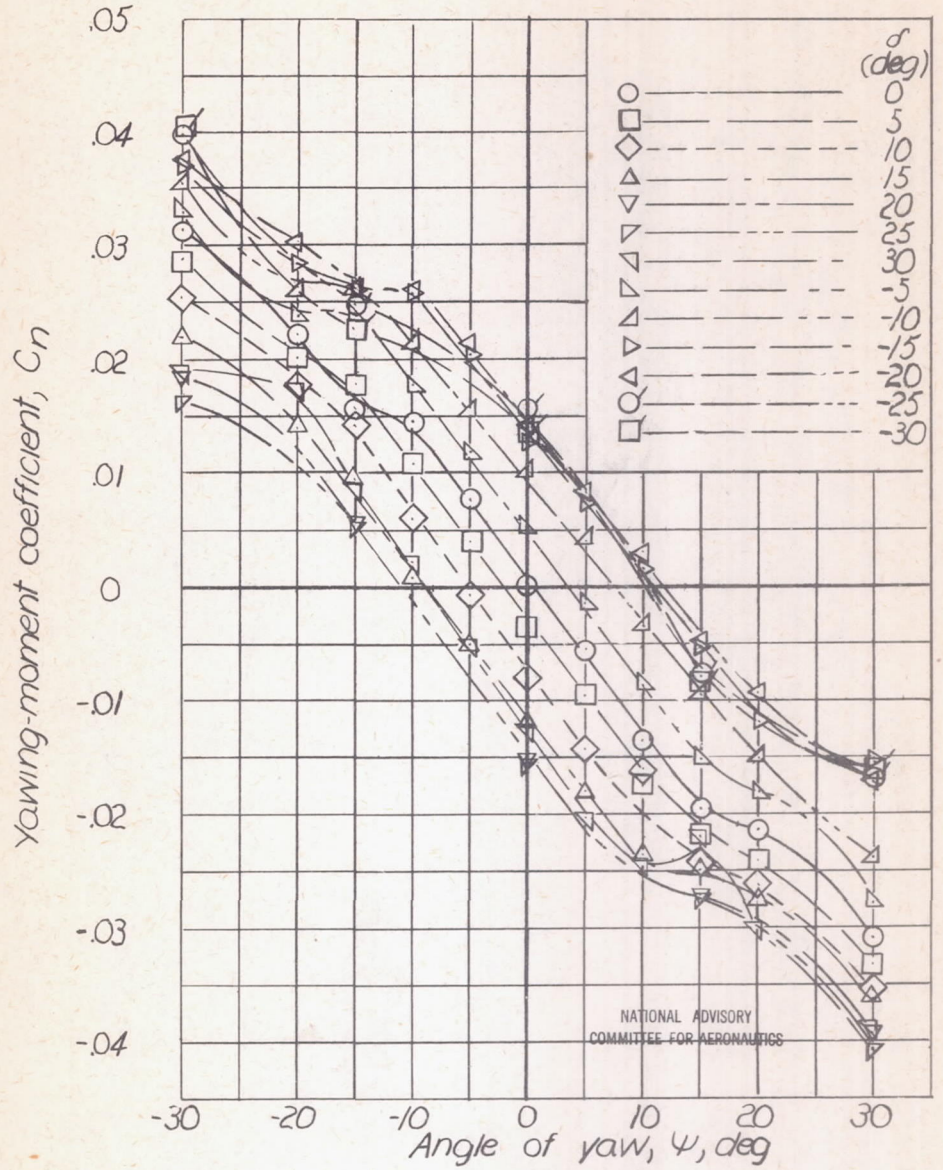

Figure 8. – Rudder effectiveness for rudder 3.

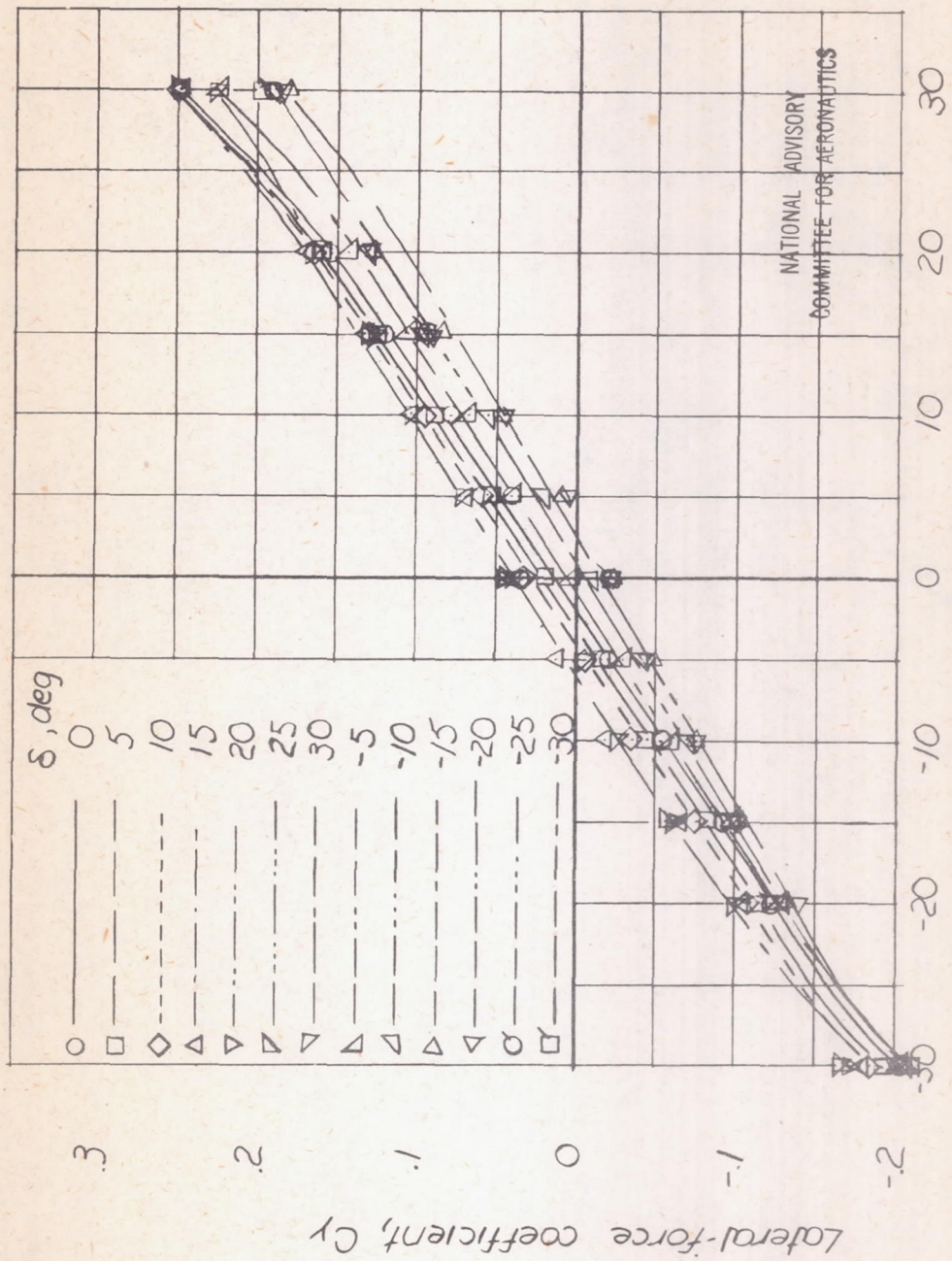

Figure 8. - Concluded.

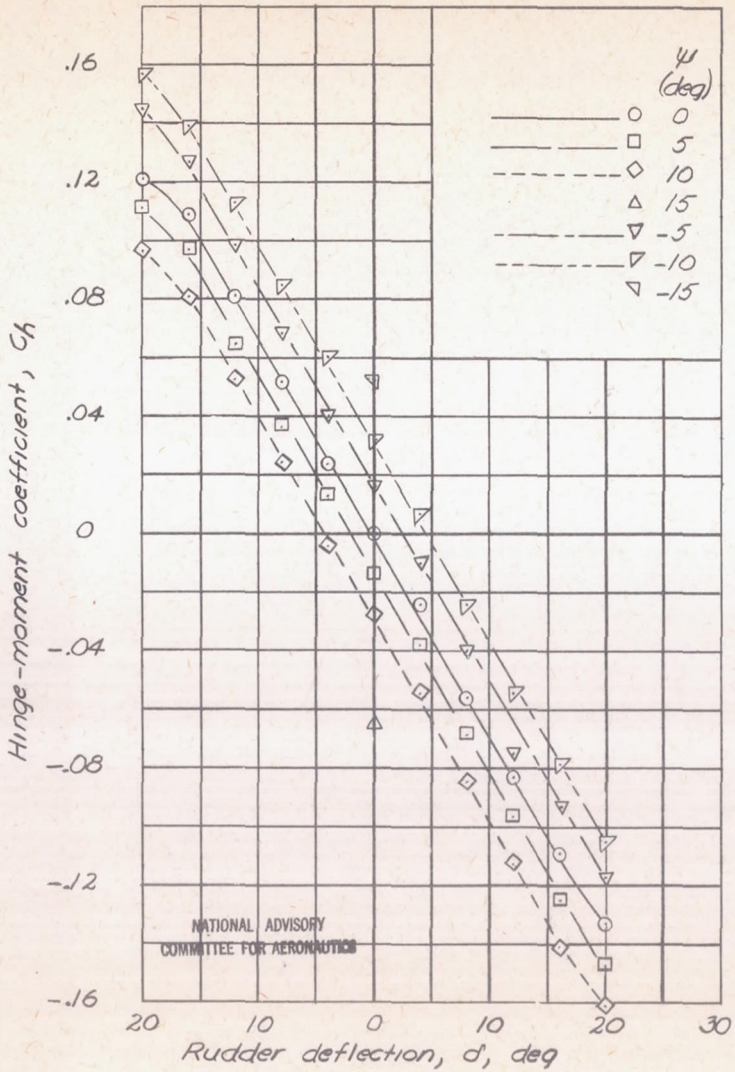

Figure 9.- Hinge-moment characteristics of rudder 1.

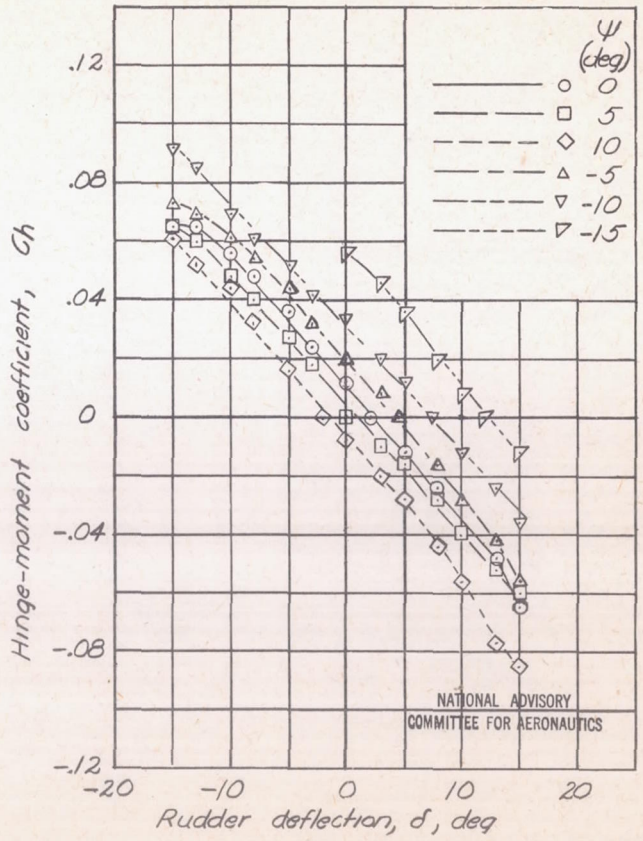

Figure 10.- Hinge-moment characteristics of rudder 2.

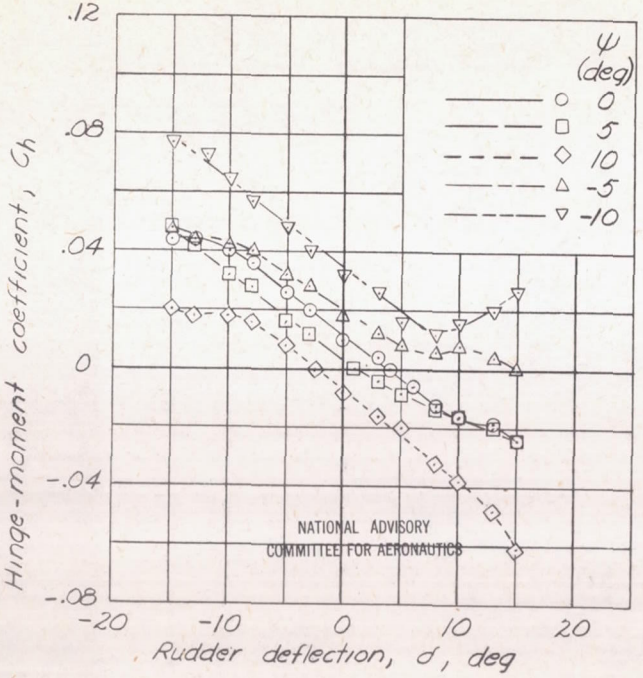

Figure 11.- Hinge-moment characteristics of rudder 3.

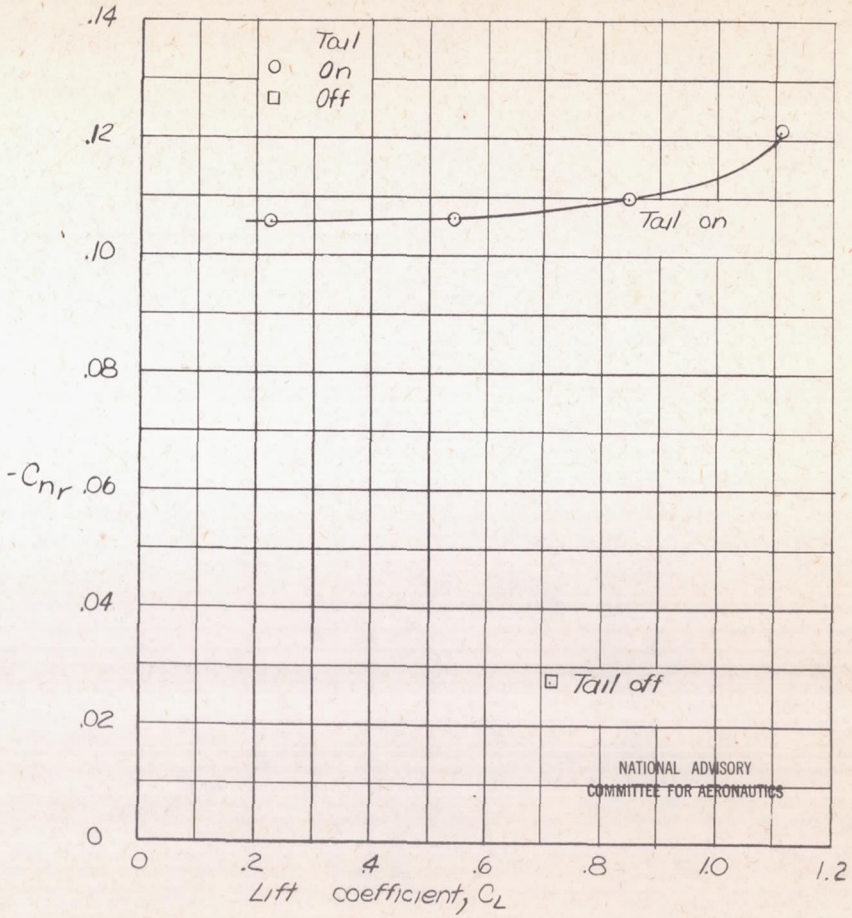

Figure 12.- Yawing-moment coefficient due to yawing for the model used in the free-flight tunnel investigation of rudder-free stability

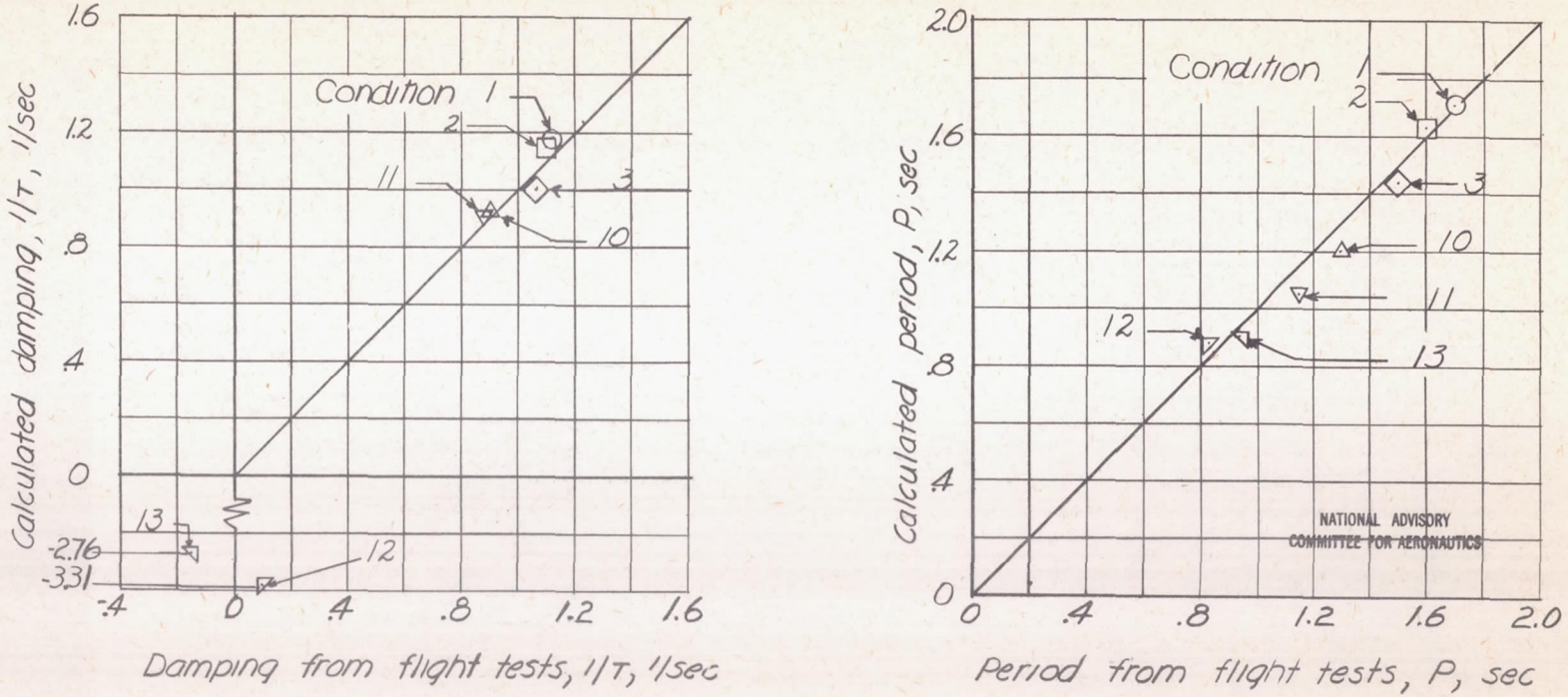

Figure 13.— Comparison of period and damping of the rudder-free oscillations of a model as calculated by the complete theory with those measured from flight tests.

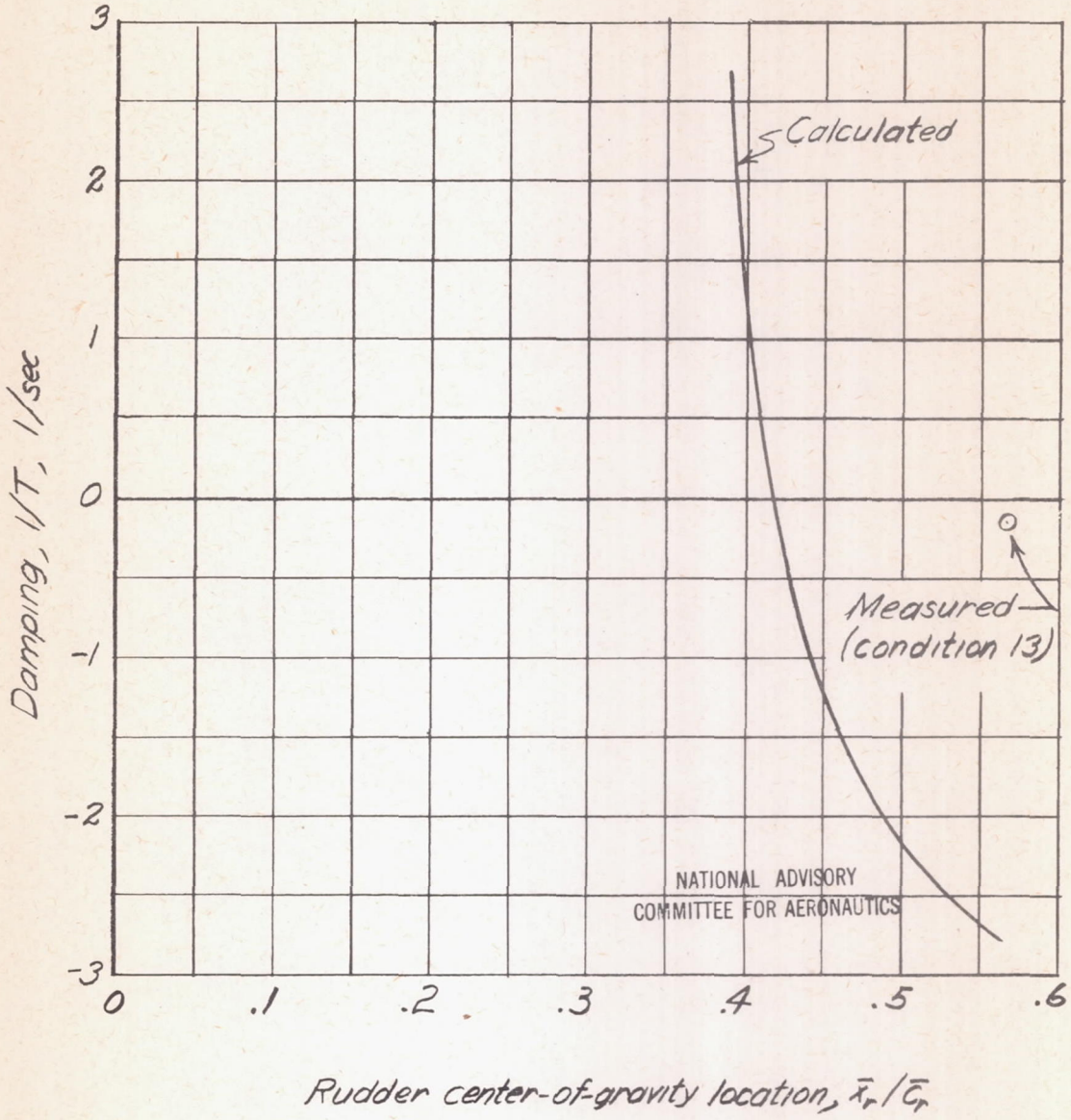

Figure 14.- Comparison of calculated and measured damping of the short-period rudder-free oscillation.

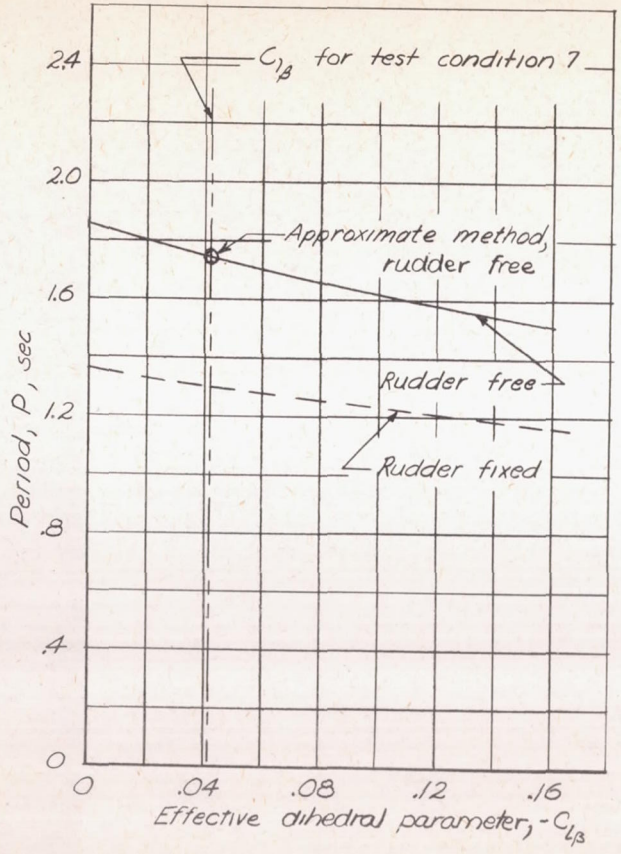

NATIONAL ADVISORY COMMITTEE FOR AERONAUTICS.

Figure 15.- Comparison of the variation of the period of the long-period oscillation with C_{l_β} as calculated, rudder fixed and rudder free, for test condition 7.

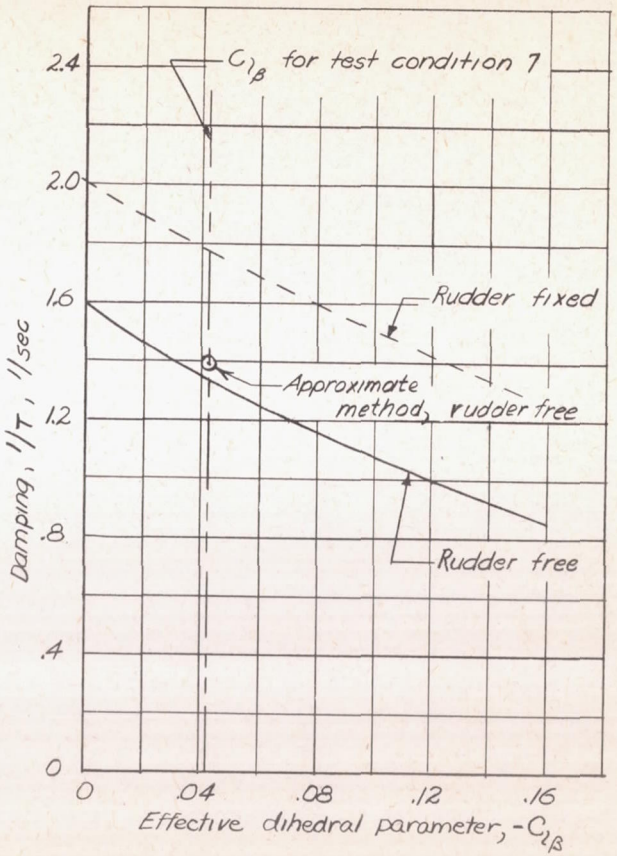

Figure 16.- Comparison of the variation of the damping of the long-period oscillation with C_{l_β} as calculated, rudder fixed and rudder free, for test condition 7.

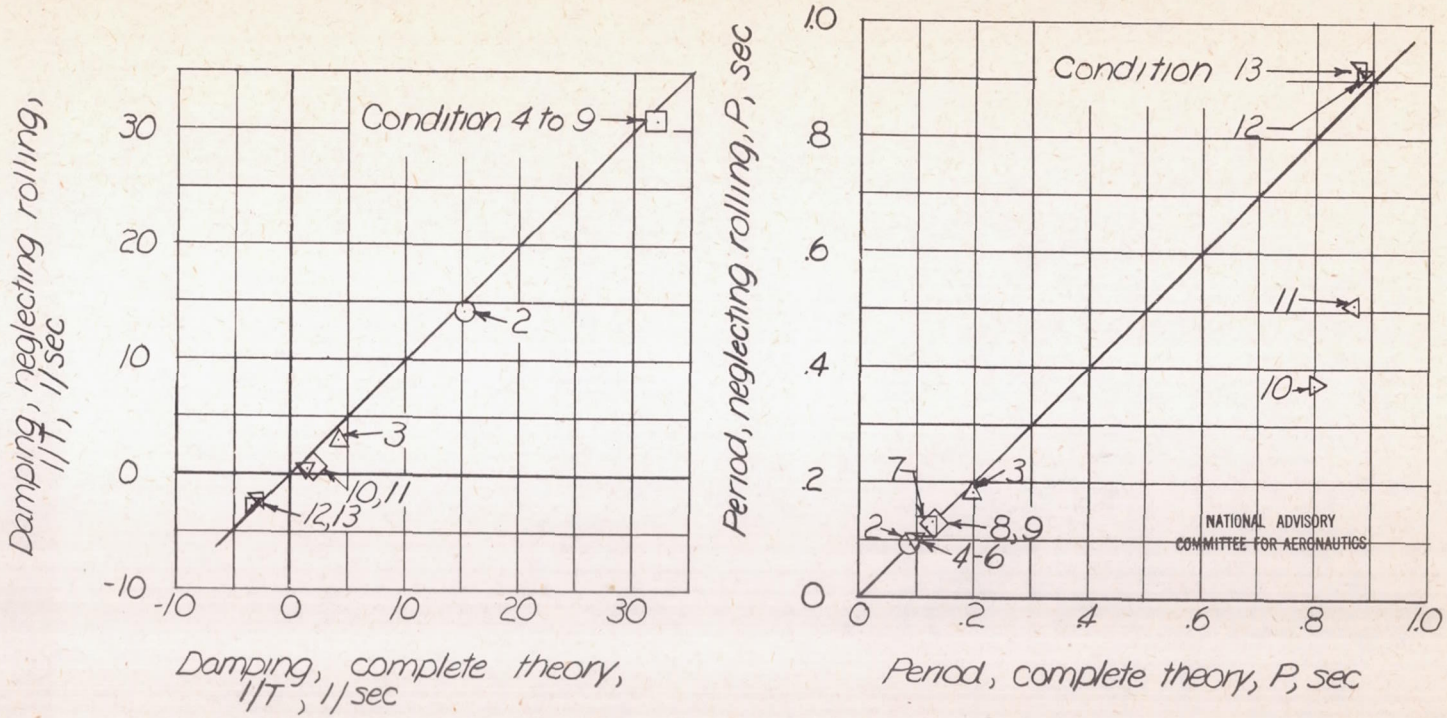

Figure 17.- Comparison of period and damping of the short-period rudder-free oscillations as calculated by the complete theory with those calculated by the theory neglecting rolling.

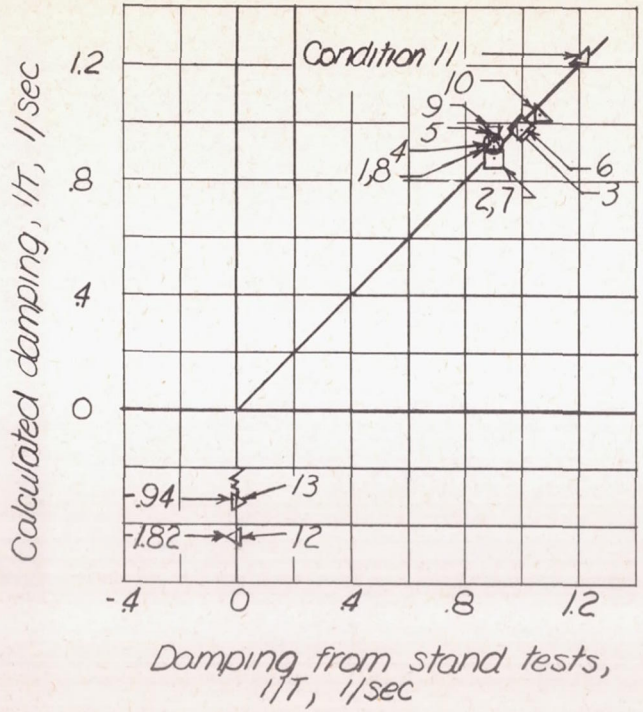

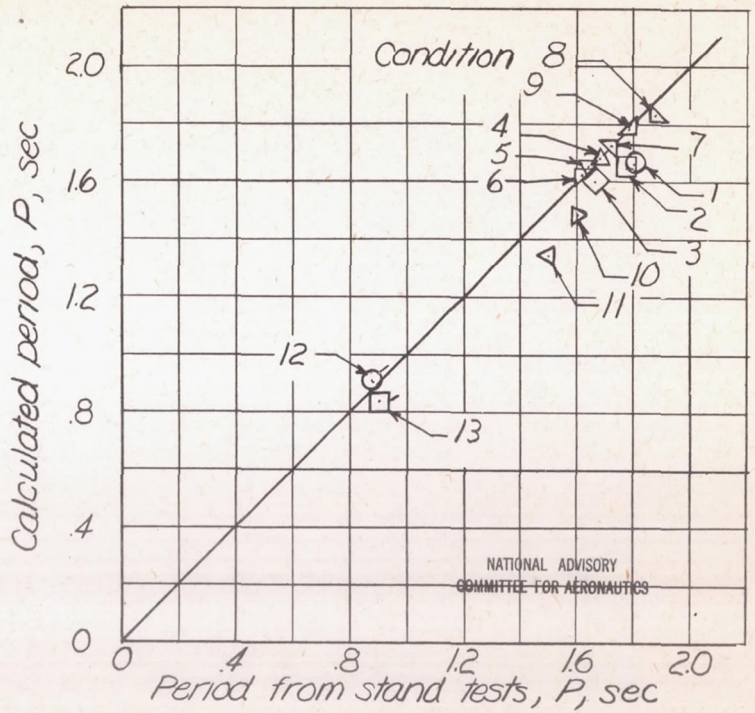

Figure 18.- Comparison of period and damping of the rudder-free oscillations of the model as calculated neglecting rolling and lateral displacement with those measured from yaw-stand tests.